Article

A dipolar cycloaddition reaction to access 6-methyl-4,5,6,7-tetrahydro-1*H*-[1,2,3]triazolo[4,5-*c*]pyridines enables the discovery synthesis and preclinical profiling of a P2X7 antagonist clinical candidate

Christa C Chrovian, Akinola Soyode-Johnson, Alexander A Peterson, Christine F. Gelin, Xiaohu Deng, Curt A. Dvorak, Nicholas I. Carruthers, Brian Lord, Ian Fraser, Leah Aluisio, Kevin J Coe, Brian Scott, Tatiana Koudriakova, Freddy Schoetens, Kia Sepassi, David J. Gallacher, Anindya Bhattacharya, and Michael A Letavic

J. Med. Chem., **Just Accepted Manuscript** • DOI: 10.1021/acs.jmedchem.7b01279 • Publication Date (Web): 06 Dec 2017

A dipolar cycloaddition reaction to access 6-methyl-4,5,6,7-tetrahydro-1*H*-[1,2,3]triazolo[4,5-*c*]pyridines enables the discovery synthesis and preclinical profiling of a P2X7 antagonist clinical candidate

Christa C. Chrovian, [*,1] *Akinola Soyode-Johnson,* [1] *Alexander A. Peterson,* [1] *Christine F. Gelin,* [1] *Xiaohu Deng,* [1] *Curt A. Dvorak,* [1] *Nicholas I. Carruthers,* [1] *Brian Lord,* [1] *Ian Fraser,* [1] *Leah Aluisio,* [1] *Kevin J. Coe,* [1] *Brian Scott,* [1] *Tatiana Koudriakova,* [1] *Freddy Schoetens,* [1] *Kia Sepassi,* [1] *David J. Gallacher,* [2] *Anindya Bhattacharya*[1] *and Michael A. Letavic* [1]

[1]Janssen Research & Development, LLC, 3210 Merryfield Row, San Diego, California 92121
[2]Janssen Research & Development, Janssen Pharmaceutica NV, Turnhoutseweg 30, 2340 Beerse, Belgium

ABSTRACT: A single pot dipolar cycloaddition reaction / Cope elimination sequence was developed to access novel 1,4,6,7-tetrahydro-5*H*-[1,2,3]triazolo[4,5-*c*]pyridine P2X7 antagonists that contain a synthetically challenging chiral center. The structure-activity relationships of the new compounds are described. Two of these compounds, (*S*)-(2-fluoro-3-(trifluoromethyl)phenyl)(1-(5-fluoropyrimidin-2-yl)-6-methyl-1,4,6,7-tetrahydro-5*H*-[1,2,3]triazolo[4,5-*c*]pyridin-5-yl)methanone (compound **29**) and (*S*)-(3-fluoro-2-

(trifluoromethyl)pyridin-4-yl)(1-(5-fluoropyrimidin-2-yl)-6-methyl-1,4,6,7-tetrahydro-5*H*-[1,2,3]triazolo[4,5-*c*]pyridin-5-yl)methanone (compound **35**), were found to have robust P2X7 receptor occupancy at low doses in rat with ED_{50} values of 0.06 and 0.07 mg/kg, respectively. Compound **35** had notable solubility compared to **29** and showed good tolerability in preclinical species. Compound **35** was chosen as a clinical candidate for advancement into Phase I clinical trials to assess safety and tolerability in healthy human subjects prior to the initiation of proof of concept studies for the treatment of mood disorders.

INTRODUCTION:

Pro-inflammatory cytokines may be a significant contributor to the pathology of psychiatric malfunctioning. Indeed, elevated levels of inflammatory biomarkers have been identified in individuals diagnosed with bipolar and major depressive disorders.[1] The P2X7 receptor is an ATP-gated ion channel involved in a prominent inflammatory cascade in central nervous system (CNS) immune cells (microglia) that results in the release of the "master" inflammatory cytokine IL-1β, so called because of its role in triggering an acute phase response.[2] P2X7 enables the release of IL-1β by converting pro-IL-1β into its mature form. In the CNS this occurs primarily in microglia and triggers a neuroinflammatory cascade. As part of our ongoing interest in the chronic effects of prolonged neuroinflammation, and in particular the role of neuroinflammation in psychiatric conditions, we have been working to advance brain-penetrant selective P2X7 antagonists into clinical proof of concept (PoC) studies in order to study the effect of inhibiting overall IL-1β release (CNS + peripheral) on individuals suffering from mood disorders. Toward this goal, we have found that P2X7 antagonists are efficacious in pre-clinical chronic models of

depression.[3] Data have also been presented suggesting that P2X7 antagonists that can cross the blood-brain barrier may be the most effective at treating psychiatric conditions.[4,5]

At least two selective P2X7 antagonists have advanced into PoC studies for the treatment of Crohn's disease (CD)[6] and/or Rheumatoid Arthritis (RA).[7,8] These two compounds -- one from Pfizer[8] and one from AstraZeneca[6,7] -- were both effective at blocking peripheral IL-1β release in ex vivo ATP-activated patient plasma samples. Neither compound ultimately met its desired clinical endpoint in the studies, and their development for either RA[7,8] and/or CD[6] was discontinued.

We recently disclosed the structure of JNJ-54175446 (**1**), which has successfully completed initial Phase I clinical studies.[9] Compound **1** is a potent P2X7 antagonist with significant brain penetration and exhibits dose-dependent P2X7 receptor occupancy in the hippocampus of rats and dogs. It is considered to be a Biopharmaceutical Classification System (BCS) Class II compound based on its high permeability and low solubility; in aqueous buffer its solubility was 39 μM at pH 2 and 21 μM at pH 7, but was found to be readily absorbed in preclinical species, with a bioavailability of ~100% in dog. The predicted human half-life of **1** was 29 h.[9]

While compound **1** progressed into preclinical development, the project team remained interested in a back-up compound with high solubility as well as differentiated absorption, distribution, metabolism and elimination (ADME) properties, specifically, one with more rapid elimination.

Throughout our work on P2X7 antagonists containing 5,6-fused cores,[10] we have found that a 4*R*-methyl (as in **1**[9] and **2**[11]) or –phenyl (as in **3**)[12] substituent provides improved potency compared to an unsubstituted 4-position,[10,13] particularly in rodent species. The added 4*R*-substituent also provided improved microsomal stability[9,11] and decreased CYP2C19 inhibition.[9]

The recent report describing compound **1** establishes that a methyl 4*R*-orientation is the preferred epimer for P2X7 potency of 4-methyl-4,5,6,7-tetrahydro-1*H*-[1,2,3]triazolo[4,5-*c*]pyridines.[9] Separately, we have shown that 6-methyl groups also provide benefit in fused ring cores (**4**[14] and **5**[15]), and the stereochemistry was determined to be *S* in the examples for which an assignment was conclusively made, including **4**[14] and 1-(5,6-dihydro-[1,2,4]triazolo-[4,3-*a*]pyrazin-7(8*H*)-yl)methanones[10]. It should be noted that while the absolute configuration of **5** was not determined, the specific rotation value was positive.[15] The 6*S*-methyl group had been underexplored with 4,5,6,7-tetrahydro-1*H*-[1,2,3]triazolo[4,5-*c*]pyridine cores. We thus became interested in investigating (*S*)-6-methyl-1,4,6,7-tetrahydro-5*H*-[1,2,3]triazolo[4,5-*c*]pyridines.

Chart 1. Fused triazole and pyrimidine core P2X7 antagonists containing a C-methyl or -phenyl substituent in the piperidine or piperazine ring.

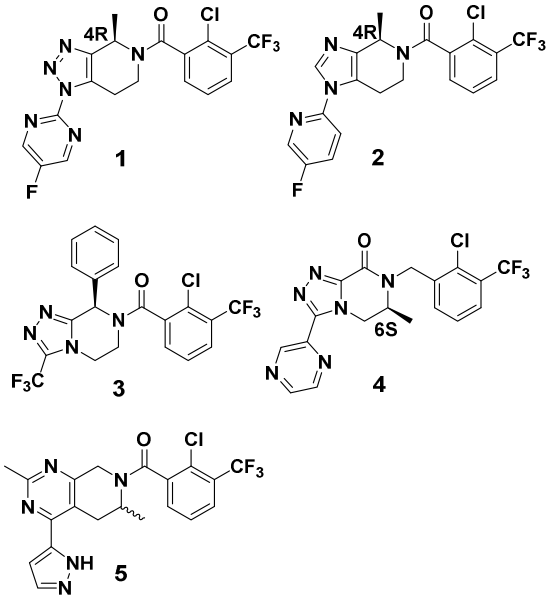

RESULTS AND DISCUSSION:

Synthetic Methodology Development. One challenge in executing this proposal was devising synthetic methods for the rapid assembly of final compounds. Compelling 1,2,3-triazole syntheses includes click chemistry of an alkyne and an azide.[16] In our case of a fused triazole, this would be followed by elaborating the 5-position of the ring with functionality that could,

after a ring closing reaction with a 4-methylamino group, form the fused triazole system (Scheme 1, eq A).[17] However, this strategy is rarely used with Het- or aryl- azides, and becomes more challenging given the 6-methyl group we needed to install.[17-19] In an alternative method, the fused triazole can be formed from a diaminopyridine, which is followed by a reduction of the pyridine ring (eq B).[13,20] Both of these routes require several challenging steps. With the required absolute configuration, the synthesis becomes additionally arduous. We were interested in developing a concise route to enable rapid access to the 1-Het-6*S*-methyl-1,4,6,7-tetrahydro-5*H*-[1,2,3]triazolo[4,5-*c*]pyridines, and thought that a 1,3-dipolar cycloaddition of an azide and a ketone was worth investigating.

Scheme 1. Synthetic methods for the preparation of 1-Het-1,4,6,7-tetrahydro-5*H*-[1,2,3]triazolo[4,5-*c*]pyridines.

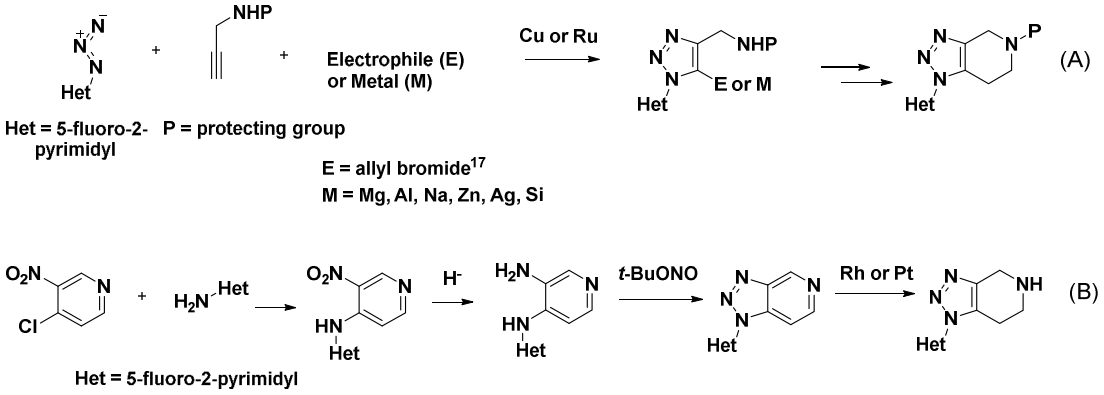

As early as 1967, Huisgen et al. reported 1,3-dipolar cycloadditions with azides and an enamide that could form triazoles in a fused ring system.[21] This reaction has been more recently elaborated using ketones and azides in the presence of an amine organocatalyst. In one example, Ramachary and co-workers reported the use of activated ketones in an enamine amination / elimination followed by [3+2]-cycloaddition / hydrolysis in an organocatalytic cascade as a synthetic approach to substituted-1,2,3-triazoles (Scheme 2, eq A).[22] Perhaps more relevant to our work is the cascade reaction using unactivated ketones reported in 2011 by Belkheira et al.[23] In this work, carbocyclic ketones were reacted with aryl azides, presumably via enamine

formation, in a dipolar cycloaddition reaction (Scheme 2, eq B). We hoped we could extend this methodology to the formation of 6-methyl-4,5,6,7-tetrahydro-1*H*-[1,2,3]triazolo[4,5-*c*]pyridines from unsymmetrical ketone heterocycles containing a chiral center (Scheme 2, eq C). We kept in mind however, that the altered electronics and added steric bulk of our starting ketone (versus the literature), as well as the need for a specific regiochemical outcome, could make the optimization challenging.

Scheme 2. Synthesis of fused-1,2,3-triazoles by an enamine amination / elimination followed by [3+2]-cycloaddition / hydrolysis organocatalytic cascade.

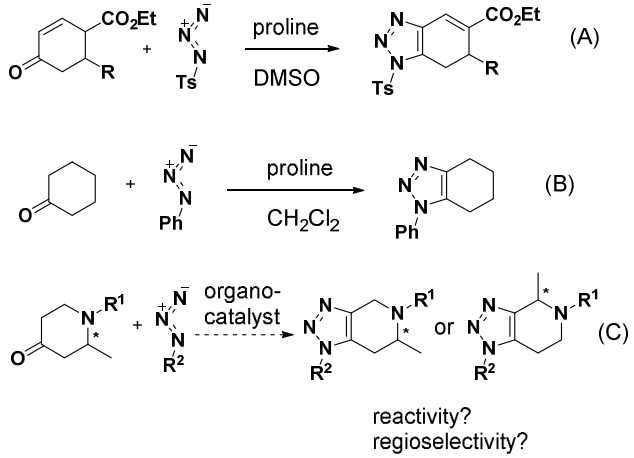

Initial investigations were conducted using phenyl azide and ketone rac-**6** following the protocol reported by Belkheira et al.[23] We found that the reaction did not proceed with **6** using their optimized conditions of catalytic proline and CH_2Cl_2 solvent (Table 1, entry 1). We found that when pyrrolidine was used instead of proline, the reaction proceeded, albeit in low yields (entry 2). However, the products that were isolated contained a pyrrolidine adduct (**7a** and **8a**), which we supposed was an intermediate that could be readily converted to desired product. It was not surprising that the yield improved when a full equivalent of pyrrolidine was used (entry 3). Comparable yields were achieved with ethanol solvent (entry 4), and were higher using toluene (entry 5).

Table 1. Initial results of a dipolar cycloaddition with 2-methylpiperidone and phenyl azide.

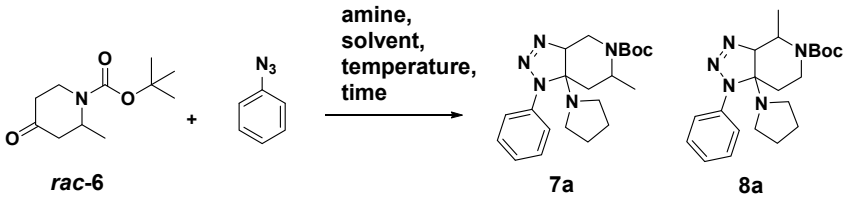

rac-**6** **7a** **8a**

entry	amine	solvent	conditions	isolated yield
1	proline, catalytic	DCM	rt or 80 °C microwave	no reaction
2	pyrrolidine, catalytic	DCM	80 °C microwave	<5% **7a**+**8a**[a]
3	pyrrolidine, 1 equiv	DCM	80 °C microwave	34% **7a**+**8a** (1:1)
4	pyrrolidine, 1 equiv	EtOH	120 °C microwave	29% **7a**+**8a** (1:1)
5	pyrrolidine, 1 equiv	toluene	100 °C	63% **7a**+**8a** (1:1)

[a] In these examples, the yields and relative ratios of **7a** and **8a** were not rigorously determined.

Unfortunately, attempts to facilitate an acid catalyzed elimination of **7a** + **8a** to form **9a** + **10a** were unsuccessful using either catalytic or stoichiometric amounts of *p*-TSA. One thought we had was to use oxidative conditions in order to set up a Cope elimination. Gratifyingly, after treating an isolated mixture of **7a** + **8a** (1:1) with *m*-CPBA, a rapid transformation occurred to form **9a** + **10a** in a 1:1 ratio and 83% isolated yield (Scheme 3). In fact, this elimination could even be conducted in a single pot format, following the [3+2] cycloaddition step. The best overall yields for the sequence were obtained when we combined the ketone, azide and pyrrolidine at once with heating. Then, after formation of the intermediates **7** and **8** in roughly 2 hours, *m*-CPBA was added. Due to this development, our experimental procedure for forming fused triazoles was now quite simple in that three steps, i) enamine formation, ii) dipolar cycloaddition and iii) Cope elimination, are conducted in a single pot.

However, an unresolved problem remained for the formation of phenyl-substituted 6-methyl-4,5,6,7-tetrahydro-1*H*-[1,2,3]triazolo[4,5-*c*]pyridines. There was no regioselectivity for the formation of **7a** versus **8a**. Since the reaction appeared to have many variables that could potentially be optimized, we undertook a more detailed investigation of nitrogen protecting groups, amine bases, solvents and temperatures.

Scheme 3. Pyrrolidine adduct elimination via oxidation and Cope elimination.

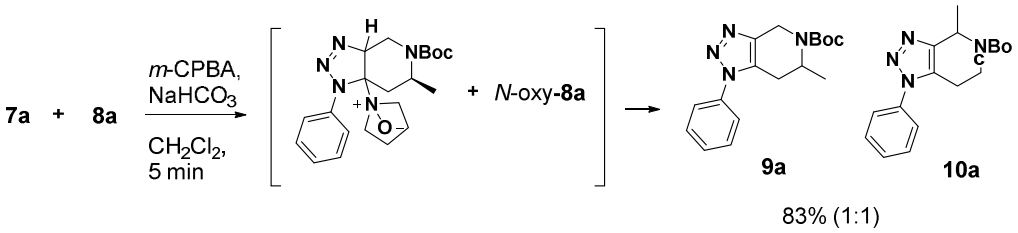

The next reaction optimizations were conducted using 2-azido-5-fluoropyrimidine (the same pyrimidine featured in **1**) and *N*-protected 2-methyl-piperidones (Table 2). A solvent and temperature screen revealed that the best yields and regioselectivities were obtained at higher temperatures with toluene or 1,4-dioxane (entries 1-6). Dean-Stark conditions had minimal impact on the regioselectivity and yield (entry 7). It is interesting to note that using phenyl azide under the best reaction conditions resulted in a significantly lower regioselectivity than when the fluoropyrimidine azide was used (compare entry 6, Table 2 (88:12) with entry 5, Table 1 (1:1)). This is a curious and unexpected finding. One possible reason for this could be that the electron deficiency of the fluoropyrimidine azide favors a thermodynamic product by enabling reversibility, although this hypothesis has not been tested. The nitrogen protecting groups were also screened, and carbamate protecting groups worked well but *N*-methyl and -benzyl groups resulted in no reaction (entries 8-11). A screen of secondary amines appeared to favor the use of unsubstituted pyrrolidine (a subset of amines is shown in entries 12-16). Proline once again did not promote the reaction (entry 14).

Table 2. One pot dipolar cycloaddition / Cope elimination reaction optimization using 2-azido-5-fluoropyrimidine.

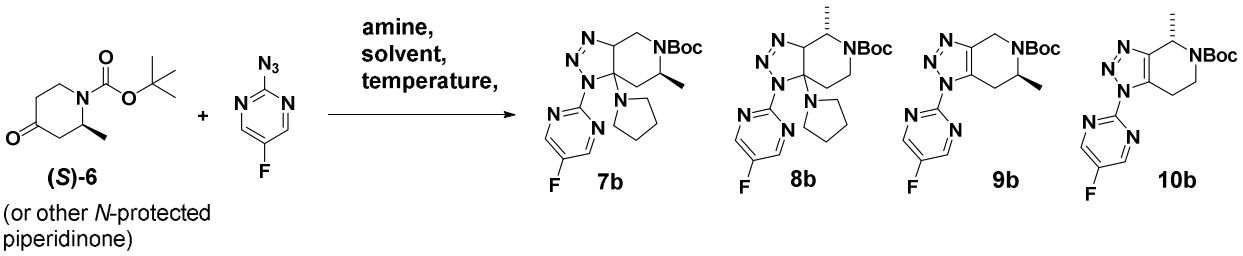

Entry	*N*-protected piperidinone	amine (1 equiv)	solvent	temp	yield, **9b**:**10b**[a]
1	6	pyrrolidine	toluene	100 °C	65%, 88:12[b]
2	6	pyrrolidine	EtOH	80 °C	47%, 85:15
3	6	pyrrolidine	MeCN	80 °C	37%, 82:18
4	6	pyrrolidine	1,4-dioxane	100 °C	62%, 89:11
5	6	pyrrolidine	TFE	80 °C	0% of **9b** or **10b**[c]
6	6	pyrrolidine	toluene	rt	19%, 60:40
7	6	pyrrolidine	toluene	reflux 4h Dean-Stark	60%, 88:12
8	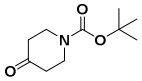	pyrrolidine	toluene	100 °C	59%
9	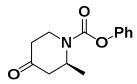	pyrrolidine	toluene	100 °C	48%, 7.5:1
10	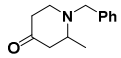	pyrrolidine	toluene	100 °C	no reaction
11		pyrrolidine	toluene	100 °C	no reaction
12	6		toluene	100 °C	no reaction
13	6		toluene	100 °C	no reaction
14	6		toluene	100 °C	no reaction
15	6		toluene	100 °C	no reaction
16	6		toluene	100 °C	no reaction

[a] Reported as isolated yield of the mixture of regioisomers.
[b] The result is the average yield of n=5 reactions.
[c] Byproducts were observed but not characterized.

The scope of the reaction was next investigated using a variety of carbo- and hetero- cyclic ketones, as well as aryl and alkyl azides. The reaction's utility is enhanced by the fact that both aromatic and alkyl azides were reactive. All of the reactions in Table 3 were conducted using commercially available azides. The highest yields were with phenyl azide and carbocyclic or *N*-heterocyclic ketones (**11-13**), an exception being 5-membered ring ketones which did not react to form product (**14** and **17**). *tert*-Butyl 4-oxoazepane-1-carboxylate reacted to form the two possible regioisomeric products with roughly equal preference (1:1 for **13a**:**13b** and 1:2 for **23a**:**23b**). The oxygen- and sulfur-containing ketones reacted in low to moderate yields (**15-16** and **24-25**). Products **18-20** are examples from reactions using different aromatic azides, and low to moderate yields were obtained in these cases as well. It should be noted however, that despite low to moderate yields obtained, the ability to form a fused triazole ring system using a variety of functionalized azides is an excellent option for medicinal chemists at the hit-to-lead or lead optimization stage of a program, where facile access to relevant substrates is of high value in order to quickly evaluate structure-activity relationships (SAR).

Table 3. Screen of cyclic ketones in the dipolar cycloaddition / Cope elimination using aryl or alkyl azides.

pdt	ketone	azide	pdt structure	Yield[a]	pdt	ketone	azide	pdt structure	Yield[a]
11	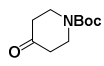	N_3-Ph	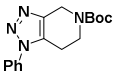	66%	19	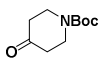	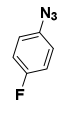	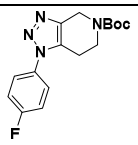	41%[b]
12		N_3-Ph		59%	20	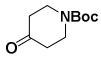	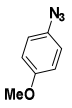	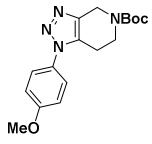	13%
13a 13b		N_3-Ph	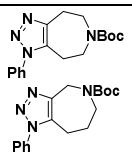	63%, 1:1	21	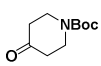	N_3-*i*Pr	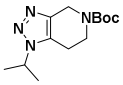	55%
14		N_3-Ph	no reaction	--	22		N_3-*i*Pr		38%

15		N_3-Ph		25%	23a 23b	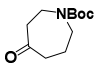	N_3-*i*Pr	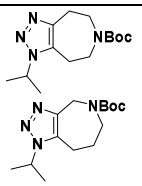	43%, 1:2
16		N_3-Ph		8%	24		N_3-*i*Pr		ND[a]
17		N_3-Ph	no reaction	--	25		N_3-*i*Pr		18%[b,c]
18		N_3-Bn	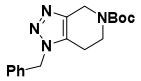	38%					

[a] Reported as isolated yield.
[b] The yield is the average range of several reactions.
[c] The product mass was observed not isolated.

SAR of (1)-(6*S*-methyl-1,4,6,7-tetrahydro-5*H*-[1,2,3]triazolo[4,5-*c*]pyridin-5-yl)methanones. At this point we were eager to apply the [3+2] cycloaddition / Cope elimination method to the synthesis of the desired 6-methyl-1,4,6,7-tetrahydro-5*H*-[1,2,3]triazolo[4,5-*c*]pyridine core in order to evaluate P2X7 SAR. After formation of the core, a Boc-deprotection followed by amide bond formation gave the desired final compounds. Compounds **26-29** and **32-40** in Tables 4 and 5 were synthesized using this method.

We began with 2,3-substituted benzamide analogs in order to evaluate SAR of different *N*-aryl triazole substituents. This choice was made due to previous work that established 2,3-halo,-alkyl, and -haloalkyl groups to be preferred substituents on the benzamide moiety of 5,6-fused core P2X7 antagonists.[9-15,24] We focused almost exclusively on the 6*S*-methyl configuration based on earlier findings as well with related cores; all of the 6*R*-methyl epimers prepared and tested on 6,6- and 5,6-fused cores had poor P2X7 potency.[10,14-15]

Shown in Tables 4 and 5 are IC_{50} values of the final compounds as measured in a calcium mobilization assay, as well as their in vitro CYP inhibition, solubility and liver microsomal

turnover extraction ratios (ER). Compounds **26-34** contain a 2-chloro, -fluoro or -methyl substituted 3-trifluoromethyl phenyl amide and the fused triazole is *N*-linked to a pyridine, pyrazine, pyrimidine or pyrazole (substituted or unsubstituted) group. They all demonstrated good human P2X7 potency with IC_{50} values of 1.7-19 nM. In rat, IC_{50} values were also < 20 nM, with the exception of **33** (rP2X7 IC_{50} = 404 nM). In this set of compounds, CYP2C19 and 2C9 inhibition was prevalent, although **29** showed no significant inhibition of any of the six CYP isoforms tested.

Many of the compounds in Table 4 have low solubilities. In addition, compounds **26** and **30-34** had poor stability in vitro human and rat liver microsomes. The compounds that demonstrated higher stability in liver microsomes have a 5-fluoropyrimidine-substituted triazole (**27-29**). The electron deficiency of this moiety might explain its lower propensity for oxidative metabolism as compared to the other heteroaromatic groups.

Table 4. In vitro data for 1-(6*S*-methyl-1,4,6,7-tetrahydro-5*H*-[1,2,3]triazolo[4,5-*c*]pyridin-5-yl)methanone P2X7 antagonists with 2-R^2,3-(trifluoromethyl)phenyl substituents.

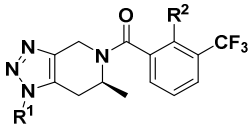

cpd	R^1	R^2	hP2X7 IC_{50} (nM)[a]	rP2X7 IC_{50} (nM)[a]	CYP IC_{50} (μM)[b]	solub pH 2/7 (μM)	extraction ratio h/r[c]
26		Cl	8.0±1.1	10±3.7	2C19 = 0.3 2C9 = 1.6	10 / 18	0.94 / 0.85
27		Cl	1.9±1.1	4.1±0.65	2C19 = 3.4	16 / 9	0.50 / 0.32
28		CH_3	14±2.4	13±5.5	2C19 = 4.3	15 / 19	0.35 / 0.54
29		F	4.8±1.1	5.9±1.0	>10	22 / 25	0.47 / 0.37

30		Cl	1.7±0.41	1.8±0.42	2C19 = 0.3 2C9=1.2	74 / 29	0.95 / 0.90
31		Cl	7.3±2.2	2.1±0.60	2C19 = 0.5 2C9 = 5.5	155 / 5	0.85 / 0.77
32	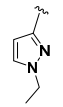	Cl	1.8±0.37	1.9±0.54	2C19 = 2.5 2C9 = 2.5	123 / 112	>0.95 / >0.92
33		Cl	19±12	404±157	2C19 = 2.6	261 / 361	0.83 / 0.89
34		Cl	2.0±0.53	10±3.0	2C19 = 0.4 2C9 = 3.7	nd	>0.95 / >0.92

[a] IC_{50} values were determined by a calcium mobilization assay in 1321N1 cells expressing the recombinant human or rat P2X7 channel and values reported are the mean of three experiments, unless otherwise stated. H is human, r is rat. All data are reported as the mean value of 3-4 assays run in triplicate; IC_{50}'s ± SD are reported.

[b] CYP IC_{50} values were obtained in human liver microsomes using a "cocktail" of CYP-selective probes for the six isoforms: 1A2, 2C19, 2C8, 2C9, 2D6, 3A4.

[c] Stability in human and rat liver microsomes. Data is reported as extraction ratios where predicted hepatic clearance is divided by the species specific hepatic blood flow.

Compound **29** demonstrated good potency and ADME properties worthy of progressing. Still, we continued our SAR exploration by introducing isonicotinamides in place of the benzamide with the thought that we could effect physicochemical properties of the substrates, solubility in particular, and alter their absorption, distribution, metabolism and excretion (ADME) properties (Table 5). Compounds with chloro- or fluoro- substituents in the 3-position of the isonicotinamide were found to be potent both in human and in rat (**35-36**,**39-40**), whereas the 3-methyl analog was potent in human but not in rat (**37**). A trifluoromethyl-substituted pyrazole (**38**) had poor P2X7 potency (human IC_{50} = 4034 nM; rat IC_{50} = 2889 nM).

The compounds containing isonicotinamides showed excellent aqueous solubility as compared to the benzamide analogs (**35** vs **29**, **37** vs **28**, **36** vs **27**). This improved solubility is likely aided by a decrease in measured partition coefficient at pH 7.4 (Log $D_{7.4}$) for **35** (1.65) versus **29**, (2.23). The isonicotinic nitrogen is not basic, however, due to the strongly deficient amide. In an

ionization constant (K_a) assay with **35**, no dissociation was measured in the pH range of 2 to 12. It also may be that a disruption to crystal packing contributes to the superior solubility of **35**. Nevertheless, compound **35** also has superior solubility as compared to lead clinical candidate **1**, which is an advantage for both formulation work as well as intestinal absorption in preclinical and clinical studies.

The isonicotinamides also helped to improve metabolic stability as well as reduce CYP2C19 inhibition. Introducing a pyrazole, pyridine or pyrazine to the 1-Het position improved compound solubility (**30-33**), but these compounds are unstable in liver microsomes and inhibit CYP2C9 and CYP2C19.

Overall compounds **29** and **35** had the most promising in vitro profile and the appeal of **35** was augmented by its excellent solubility. The two compounds were advanced to in vivo evaluation.

Table 5. In vitro data for 1-(6*S*-methyl-1,4,6,7-tetrahydro-5*H*-[1,2,3]triazolo[4,5-*c*]pyridin-5-yl)methanone P2X7 antagonists with nitrogen-containing aromatic amides.

cpd	structure	hP2X7 IC_{50} (nM)[a]	rP2X7 IC_{50} (nM)[a]	CYP IC_{50} (μM)[b]	solubility pH 2/7 (μM)	extraction ratio h/r[c]
35	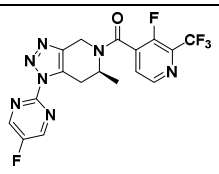	10±3.7	15±7.4	>10	>400	<0.3/ <0.2
36	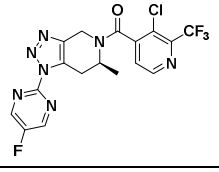	12±6.8	9.4±0.98	2C19 = 5.1	>400	<0.3 / <0.2
37	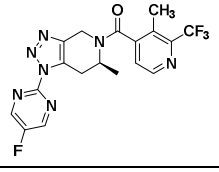	26±14	6199±837	>10	51 / >400	<0.3 / <0.2
38	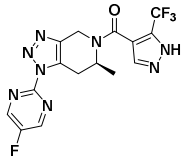	4034±740	2889±957	nd	nd	nd

39	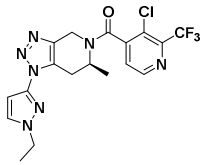	11±2.6	12±0.95	nd	nd	0.85 / 0.72
40	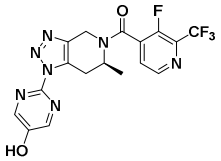	14±2.9	40±2.8	nd	nd	nd

[a] IC_{50} values were determined by a calcium mobilization assay in 1321N1 cells expressing the recombinant human or rat P2X7 channel and values reported are the mean of three experiments, unless otherwise stated. Hu is human, r is rat. All data are reported as the mean value of 3-4 assays run in triplicate; IC_{50}'s ± SD are reported.

[b] CYP IC_{50} values were obtained in human liver microsomes using a "cocktail" of CYP-selective probes for the six isoforms: 1A2, 2C19, 2C8, 2C9, 2D6, 3A4.

[c] Stability in human and rat liver microsomes. Data is reported as extraction ratios where predicted hepatic clearance is divided by the species specific hepatic blood flow.

Ex Vivo Receptor Occupancy Studies in Rat. Compounds **29** and **35** were next assessed in a receptor occupancy duration of action study measured by ex vivo autoradiography to determine P2X7 target engagement in the rat brain. Six animals were dosed 10 mg/kg p.o., **29** as a suspension and **35** as a solution, and receptor occupancy was measured at three time points. The brain versus plasma ratios of **29** and **35** were found to be approximately 1:1 or greater at the three time points, indicating high brain distribution for both compounds (Table 6). The 10 mg/kg dose resulted in ≥90% occupancy for both compounds at the 6-hour time point. The two compounds were next evaluated in a dose-response receptor occupancy study where they performed especially well, with ED_{50} P2X7 occupancy values of 0.06 mg/kg and 0.07 mg/kg for **29** and **35**, respectively, in the rat brain (Figure 1). These ED_{50}s corresponded to brain/plasma EC_{50} values of 19/16 and 12/15 ng/mL for **29** and **35**, respectively. (The concentrations are the sum of plasma protein bound and unbound fractions).

The data for compounds **29** and **35** compared favorably with previous P2X7 antagonists, as measured by the efficacious doses in rat (Table 7). The compounds in Table 7 represent six different structural classes of compounds, and their ED_{50} values were all generated using the same radiotracer in the receptor occupancy dose response assay.[9,11-14] Of this set, a 6,6-fused core compound (**5**) has the lowest EC_{50} values. However, its preclinical pharmacokinetic (PK) data from 3 species translated to a relatively high human dose prediction.[15] Compound **4** also had promising EC_{50} receptor occupancy data, however its rat ED_{50} was 10-fold higher than for compounds **29** or **35**. Ameriks et al. suggests that brain uptake of **4** is perhaps limited by efflux mechanisms, based on its unbound brain-to-plasma partition ratio ($K_{p\ u,u}$) of 0.51.[14] Compounds **2** and **3** also demonstrated inferior ED_{50}s and EC_{50}s compared to **29** and **35**. Compound **1** has advanced as the lead.[9] We continued to profile **29** and **35** as potential back-up compounds.

Table 6. Plasma and brain levels, and ex vivo P2X7 occupancies of 29 and 35 in rat hippocampus at three time points after a 10 mg/kg oral dose.[a]

	plasma levels in ng/mL			brain levels in ng/mL			P2X7 % occup.
	0.5 h	2.0 h	6.0 h	0.5 h	2.0 h	6.0 h	6.0 h
29	854.9 ± 46	1882 ± 103	1046 ± 104	1056 ± 131	2388 ± 597	1620 ± 480	95 ± 1
35	3194 ± 275	3430 ± 195	2437 ± 361	3045 ± 292	2911 ± 32	1993 ± 212	96 ± 1

a Mean ± SEM (n= 2)

Figure 1. **Dose dependency of P2X7 occupancy of 29[a] and 35[b] as measured 2h after oral administration, as measured in rat brain sections using ex vivo receptor autoradiography.[c]**

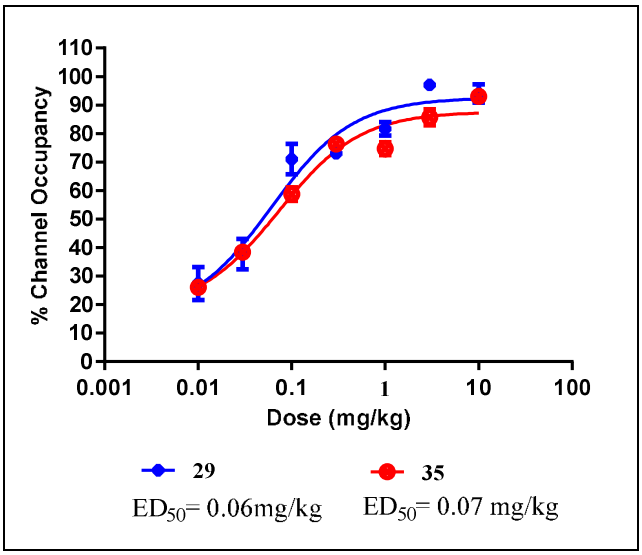

[a] 0.5% HPMC suspension

[b] 20% HP-β-cyclodextrin solution

[c] Mean ± SEM (n= 3)

Table 7. Comparison of ED_{50} values at 2h of previously reported P2X7 antagonists with 29 and 35 in ex vivo receptor occupancy studies in rat.

cpd	ED_{50} (mg)	EC_{50} brain (ng/mL)	EC_{50} plasma (ng/mL)
29	0.06	19	16
35	0.07	12	15
2[11]	2.3	362	125
4[14]	0.8	66	62
3[12]	4.3	408	748
5[15]	0.3	5	8
1[9]	0.5	108	105

Scale Up Syntheses and Characterization. Given the excellent results in the target engagement study, compounds **29** and **35** were scaled up for further studies. The synthesis of the (*S*)-1-(5-fluoropyrimidin-2-yl)-6-methyl-1,4,6,7-tetrahydro-5*H*-[1,2,3]triazolo[4,5-*c*]pyridine core was conducted using our optimized dipolar cycloaddition reaction. 2-Azido-5-fluoropyrimidine was prepared in two steps from 2-chloro-5-fluoropyrimidine and then condensed with *tert*-butyl (*S*)-2-methyl-4-oxopiperidine-1-carboxylate (commercially available in 99.7% enantiopurity) (Scheme 4). The yields of the cycloaddition / Cope elimination sequence on scales from 1 to 100 g ranged from 58 to 71%, and the ratio of regioisomers ranged from 88:12 to 91:9 in favor of the 6-methyl regioisomer. The purification of **29** was a simple wash with hot methanol to give crystalline **29** in 100% purity. The absolute configuration of the molecule was established by anomalous dispersion using the Parson's method (Figure 2).[25]

Scheme 4. Route used for both medicinal chemistry and scale-up syntheses of 29.

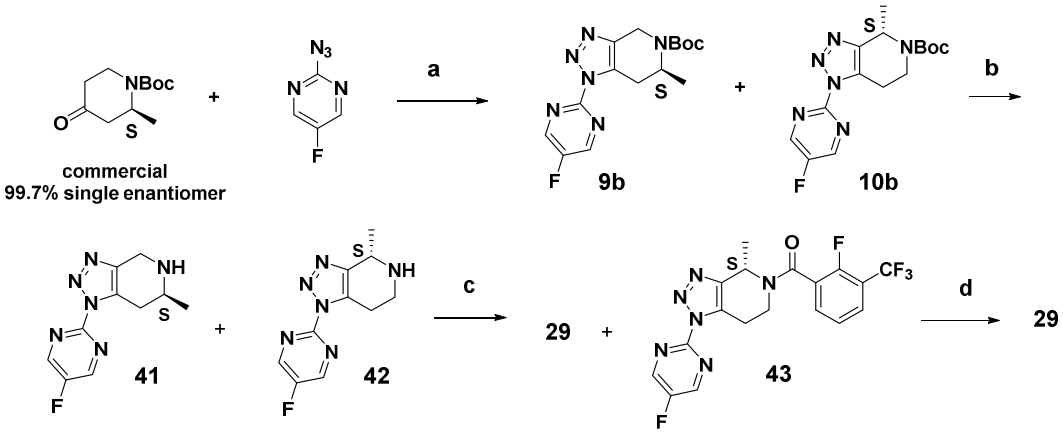

Reagents and Conditions: (a) pyrrolidine, toluene, 110 °C, 4 h; *m*-CPBA, $NaHCO_3$, rt, 10 min (58-71%, **9b**:**10b** = 9:1) (b) HCl in dioxane, CH_2Cl_2, rt, 16 h (**41**:**42** = 9:1) (c) 2-fluoro-3-(trifluoromethyl)benzoyl chloride, NEt_3, CH_2Cl_2, rt, 1 h (85% over 2 steps) (d) stir in MeOH, 60 °C, 24 h (55%, >99% ee).

Figure 2. Single crystal structure and stereochemical assignment of **29**.

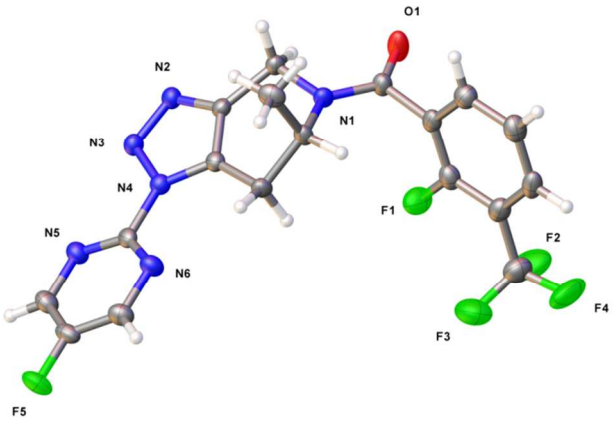

The crystallization protocol utilized to obtain pure **29** was not successful when attempted with compound **35**, because **35** is highly soluble in organic solvents and did not crystallize under a variety of conditions. In fact, in subsequent studies, identifying a stable polymorph of **35** has been unachieveable.[26] In contrast, intermediates **26** and **27** were found to be crystalline and could be separated, but due to impure or low recoveries, a slightly different route was used for the largest discovery synthesis. In this sequence, a 100 g cycloaddition / Cope elimination reaction was conducted using intermediate **44,** which has the final amide in place for the cycloaddition (Scheme 5). The reaction occurred in 69% yield, producing a 10:1 mixture of regioisomers **35** and **30**, and was followed by SFC (supercritical fluid chromatography) separation to obtain **35** in 99.5% purity. The overall yield of **35** from commercially available starting materials was 40%, and this material was used in a variety of preclinical studies.

Scheme 5. Scale-up route for the synthesis of 35.

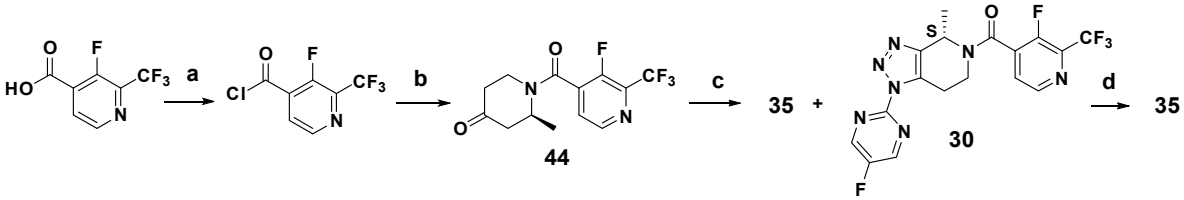

Reagents and Conditions: (a) oxalyl chloride, DMF, CH_2Cl_2, rt, 16h (b) (*S*)-2-methyl-4-oxopiperidine, NEt_3, CH_2Cl_2, rt, 1 h (77% over 2 steps) (c) 2-azido-5-fluoropyrimidine, pyrrolidine, *p*-TSA, toluene, Dean-Stark, 110 °C, 4 h; *m*-CPBA, $NaHCO_3$, CH_2Cl_2, rt, 2 h (69%, **35:30** = 10:1) (d) SFC separation, 75%.

In Vitro Studies. The key in vitro data set used to advance compounds **29** and **35** is shown in Table 8. K_i values were measured in the 1321N1 cell line overexpressing human and rat P2X7. Compounds **29** and **35** were both quite stable in human and rat liver microsomes, demonstrated insignificant inhibition of nine CYP isoforms (IC_{50}s ≥ 19 μM), as determined by measuring the effect of **29** and **35** on metabolite formation by probe substrates, and had no hERG channel inhibition up to 3 μM as measured in an automated patch-clamp assay. Compounds **29** and **35** were not found to be substrates for efflux transporters such as P-glycoprotein (P-gp) in the Caco-2 human intestinal cell line with measured efflux ratios (BA/AB) of < 2. Neither compound exhibited CYP3A4 time-dependent inhibition (TDI) in human liver microsomes, and neither induced CYP1A1/2, although **29** showed moderate activation of human PXR (66% of rifampicin control at 10 μM) and thus has the potential to induce CYP3A4. No significant activity of **29** or **35** was measured in a panel of related P2X receptors (P2X1, P2X2, P2X3, P2X2/3, and P2X4 FLIPR assays, tested up to 10 μM), and no significant binding to 50 ion channels, receptors, and transporters was detected in a commercial in vitro panel (Eurofins-CEREP, http://www.eurofins.com, tested at 10 μM). Compound **35** demonstrated moderate/low plasma protein binding in rat, dog and human (Table 8) as determined by an equilibrium dialysis method, and is considered to be a BCS Class I compound based on its high permeability and high solubility.

Table 8. In vitro ADME and selectivity data for 29 and 35.

	29	35

rP2X7 K_i [a]	1.0±0.34 nM	2.9±0.42 nM
hP2X7 K_i [a]	6.5±1.6 nM	7.1±1.9 nM
h / rat / dog / mky microsomal stability [b]	0.47 / 0.37 / <0.26 / 0.66	<0.30 / <0.20 / <0.26 / <0.19
CYP isoform IC_{50} (if IC_{50} < 50 μM)[c]	2C19 (30 μM)	2C19 (19 μM)
3A4 time-dependent inhibition	no	no
CYP induction	3A4	no
permeability (Caco-2)[d]	73/49	45/35
hERG QPatch™ IC_{50}	>3 μM	>3 μM
h / r plasma proteins (% bound) [e]	75 / 76	47 / 56

[a] K_i values are reported as the mean of 4-7 experiments in triplicate. H is human, r is rat, K_i ± SEM is reported.

[b] Stability in liver microsomes. Data is reported as extraction ratios where predicted hepatic clearance is divided by the species specific hepatic blood flow.

[c] Values were determined for CYPs 1A2, 2A6, 2B6, 2C8, 2C9, 2C19, 2D6, 2E1 and 3A4 by incubation with CYP probe substrates as described in the SI.

[d] P_{app} is reported as B-A($x10^{-6}$) cm/s / A-B($x10^{-6}$) cm/s.

[e] Plasma protein binding 0.2 μM for **35** and 0.5 μM for **29** determined by equilibrium dialysis method as previously described.[9]

Preclinical Pharmacokinetics and Human Dose Predictions. The PK of compounds **29** and **35** were investigated in preclinical species. The intravenous PK in rat, dog and monkey were characterized by low or moderate clearance (CL) and moderate volume of distribution (V_{ss}). The

high oral bioavailability (%F) measured across species was suggestive of complete absorption (Table 9).

The human CL for **29** was predicted using 3 species allometry of unbound CL corrected for in vitro CL. The human V_{ss} was predicted to be 1.9 L/kg, after correction for plasma protein binding. Based on these CL and V_{ss} values, a half-life estimate in humans was determined to be 6 hours. For a dose of 76 mg twice daily, plasma trough levels at steady state would be expected to be above the EC_{50} of 98 ng/mL over 24 h (Figure 3). The plasma concentration over time profile (Figure 3) was simulated using the predicted human PK parameters shown in Table 9.

Table 9. Pharmacokinetic data of 29 and 35 in three preclinical species.

	rat		dog		monkey		human predicted	
parameter	compound and dose (i.v. mg/kg / p.o. mg/kg)							
	29[1] 0.5 / 2.5	35[2] 1 / 5	29[1] 0.125 / 0.625	35[2] 0.25 / 1.25	29[1] 0.125 / 0.625	35[2] 0.5 / 2.5	29	35
F (%)	90	81	123	98	30	97	75	100
V_{ss} (L/kg)	2.5	1.7	2.6	1.4	1.7	1.3	1.9	1.1
CL (mL/min/kg)	12	3.7	3.8	0.8	26	2.6	4.8	0.8
$t_{1/2}$ (hr) i.v.	2.5	5.6	8.8	21.2	0.9	6.0	6	16
C_{max} (ng/mL)	541	1747	305	1123	36	1864	368	105
AUC 24h (ng/mL·h)	3190	17549	3039	23262	122	16262	5616	1786

[1] Vehicle is 50% PEG400 / 50% water

[2] Vehicle is 20% HP-β-CD

Figure 3. Simulated human plasma concentration profile of 29 at a dose of 76 mg twice daily over five days of administration.

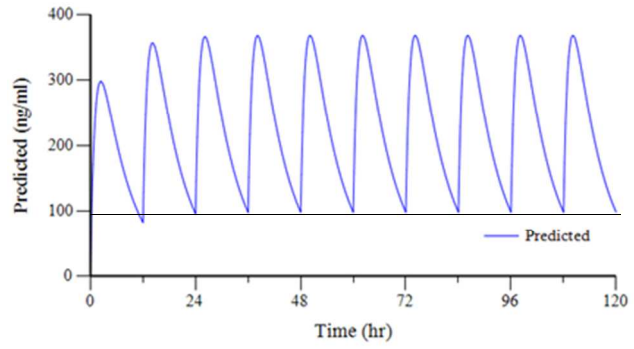

The human predictions for **35** were conducted using 3 species allometry of unbound CL[27] and V_{ss}. The human CL and V_{ss} were predicted to be 0.8 mL/min/kg and 1.1 L/kg, respectively, resulting in a predicted human $t_{1/2}$ of 16 hours. The plasma concentration over time profile (Figure 4) was simulated using the predicted human PK parameters shown in Table 8.

Figure 4. Simulated human plasma concentration profile of 35 at a dose of 6 mg once daily over six days of administration.

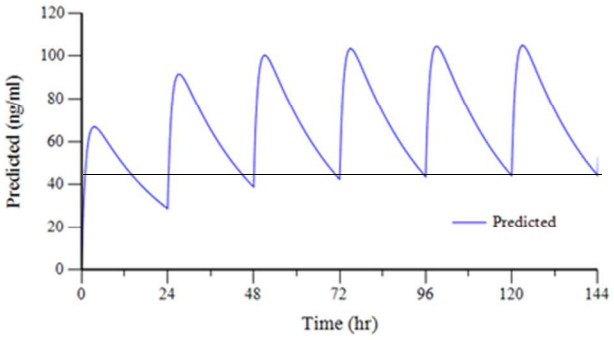

For a dose of 6 mg once daily, plasma trough levels at steady state are expected to be above the predicted EC_{50} of 45 ng/mL over 24 h, when correcting for the human vs. rat K_i value differences. The estimated C_{max} at steady state and AUC in humans for a 6 mg q.d. dose are 105 ng/mL and 1786 ng/mL·h, respectively. Given that greater blockade of IL-1β may be important for efficacy, the human dose required to maintain steady state plasma trough concentrations above the EC_{80} (225 ng/mL) was also calculated and estimated to be 30 mg q.d., with a corresponding C_{max} of 525 ng/mL and AUC of 8,930 ng/mL·h.

Based on the predicted human doses, **35** at this point appeared be the compound of choice to progress further. However, it was decided to assess both **29** and **35** in preclinical toleration in the event that **29** turned out to have a superior safety profile.

Preclinical Toleration Studies. Compounds **29** and **35** were taken into rat and dog toleration studies in order to assess their potential toxicity after oral administration, first in single dose escalation, followed by 4 or 5-day repeated dosing toleration studies. The doses selected for **29** in the 4- day study were 62.5, 125 and 250 mg/kg in rats and 35, 100, and 300 mg/kg in dogs. The doses for **29** were chosen for comparison purposes to the lead (**1**),[9] with the top doses chosen because of apparent saturation of absorption observed at higher doses in the single dose study. The doses selected for **35** in the repeated dose studies were 30, 125, 250, and 500 mg/kg/day in rats and 10, 50 and 250 mg/kg/day in dogs. The doses in dog were chosen based on exposure levels in the single dose escalation; the C_{max} and AUC were approximately the same for 250 mg/kg and 1000 mg/kg doses, thus the highest dose was not tested in the repeated dosing studies. Mortality, body weight, clinical observations, clinical pathology, gross necropsy and microscopic examination of selected tissues, toxicokinetic parameters and gene expression analysis of liver samples were evaluated.

Both compounds were well tolerated in rats and dogs. The only compound-related findings for **29** in rats were a mild increase in cholesterol (125 and 250 mg/kg) and a slight increase in total protein and albumin (250 mg/kg). In dog, there were no clinical pathology, macroscopic, or microscopic abnormalities for **29** at any dose. In rats dosed for 4 days at 250 mg/kg/day, the mean Day 4 C_{max} was 9,260 ng/mL and $AUC_{0\text{-}24h}$ was 108,000 ng·h/mL. In dogs, day 5 C_{max} at the 300 mg/kg/day dose was 5,330 ng/mL and $AUC_{0\text{-}24h}$ was 78,350 ng·h/mL.

Compound **35** exhibited higher exposures overall than **29**, increasing with dose up to 500 mg/kg in rats and 250 mg/kg in dogs. In rats, doses up to and including 125 mg/kg/day of **35** were well tolerated. Higher doses (250 and 500 mg/kg/day) were associated with adverse effects, mainly on body weight, weight gain, body temperature and neurobehavioral integrity. In dogs dosed for 5 days, there were no adverse changes at 10 mg/kg/day. Doses of 50 and 250 mg/kg/day resulted in body weight loss and lower food consumption and were associated with emesis and salivation among other clinical observations. Serum chemistry parameters (ALT, serum triglycerides and bilirubin) were also affected. Histopathological examination identified the lymphoid tissue (lymphoid depletion of the spleen and/or Peyer's patches) as target of toxicity in the high dose animals. Although histological changes were absent at the liver, this organ was nevertheless regarded as a potential target organ of toxicity because of the changes in serum chemistry. In rats dosed for 5 days at 125 mg/kg/day, the mean day 5 C_{max} was 26,000 ng/mL and $AUC_{0\text{-}24h}$ was 291,000 ng·h/mL. In dogs, the C_{max} measured on day 4 at the 10 mg/kg/day dose was 10,680 ng/mL and $AUC_{0\text{-}24h}$ was 167,000 ng·h/mL.

The maximum tolerated doses of **29** and **35** were determined in rat and dog, and used for the calculation of the predicted therapeutic index (Table 10).

Our initial requirements for advancing a second P2X7 compound into the clinic where: 1) a highly soluble compound and 2) a compound with predicted PK human parameters consistent with a predicted $t_{1/2}$ <30h. Compound **35** meets both of these criteria. In addition, the safety margins for **35** were calculated to be 5- to 10-fold higher than **29**. For these reasons, **35** was chosen for further detailed evaluation in cardiovascular and pharmacodynamic models.

Table 10. Tolerated exposures in animal studies and predicted human therapeutic levels for 29 and 35 used to calculate therapeutic index.

	rat NOAEL			dog NOAEL[c]			human predicted concentrations			predicted safety margins[d] C_{max}/ AUC	
	mg dose	C_{max}[a]	AUC[b]	mg dose	C_{max}	AUC	daily dose	C_{max}	AUC	rat/ human	dog/ human
29	250	9260	108000	300	5330	78350	152 mg	368	5616	25x C_{max}/ 19x AUC	14x C_{max}/ 14x AUC
35	125	26000	291000	10	10680	167000	6 mg	105	1786	247x C_{max} / 163x AUC	100x C_{max} / 93x AUC

[a] Units for C_{max} are ng/mL

[b] Units for AUC are ng(h)/mL

[c] Values shown are the average C_{max} and AUC for the male and female dog

[d] Human dose is predicted to translate in a 50% central P2X7 inhibition in humans

Compound **35** was taken into cardiovascular safety studies in the anesthetized guinea pig and dog. No notable electrophysiological effects were found up to the highest doses tested (associated with plasma levels of 15,500 and 12,150 ng/mL). Plasma concentrations of 2820 and 4095 ng/mL of **35** and higher in dog and guinea pig, respectively, showed increases in blood pressures. The NOAEL were 1280 and 1850 ng/mL in dog and guinea pig, respectively.

Pharmacodynamic Models. The effect of **35** on brain IL-1β release was investigated in an in vivo microdialysis assay as previously described in freely moving rats challenged with the P2X7 agonist Bz-ATP.[28] Rats were dosed orally with either vehicle or 10 mg/kg of **35** four hours prior to infusion of Bz-ATP via a microdialysis probe. Compared to vehicle, **35** significantly inhibited Bz-ATP induced IL-1β release in the rat hippocampus at the 5 and 6 h time points (Figure 5).

Figure 5. *In vivo* microdialysis assay to measure brain IL-1β levels in freely moving rats after oral administration of 10 mg/kg 35. IL-1β release was triggered by 2'(3')-O-(4-Benzoylbenzoyl)adenosine-5'-triphosphate (Bz-ATP) infusion (100 mM) in rat hippocampus. Solid line indicates time of Bz-ATP infusion (between the 4 and 6 h time

points). IL-1β concentration are given as mean values ± SEM (n= 7); P < 0.05 Robust t-test at 5 and 6 hour time points.

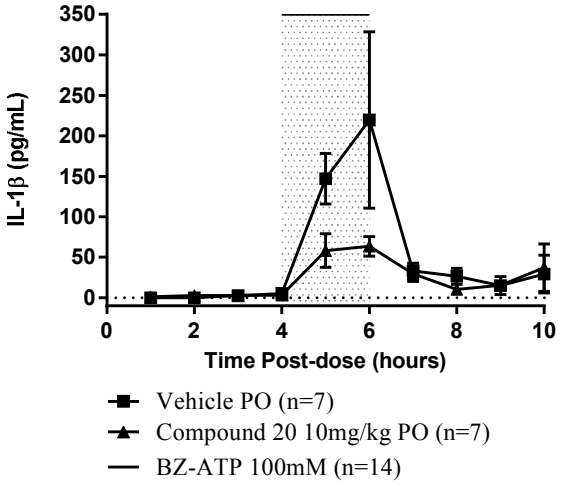

Compound **35** was also evaluated in models of depression and pain.[5] In a depression model of chronic mild unpredictable stress in rats, the animals' sucrose intake was lowered after being subjected to a chronic stress regimen for 2 weeks. Compound **35** was found to reverse this deficit.[5] The details of this model as well as the full pharmacology of compound **35** will be published in due course.

CONCLUSION:

Compound **35**, JNJ-55308942, has been chosen as the second P2X7 antagonist from Janssen to enter clinical trials, as a back-up to compound **1**. The compound was designed to have high solubility in aqueous media. This physicochemical property was achieved by incorporating an isonicotinamide moiety on a 1-(6*S*-methyl-1,4,6,7-tetrahydro-5H-[1,2,3]triazolo[4,5-c]pyridin-5-yl)methanone core. Synthetically, the preparation of the 1-((5-fluoropyrimidin-2-yl)-1,4,6,7-tetrahydro-5*H*-[1,2,3]triazolo[4,5-*c*]pyridin-5-yl)methanone core featuring the 6*S*- methyl group was foreseen to be challenging, as existing methods would have made the synthesis lengthy and

cumbersome. As such, a novel single pot dipolar cycloaddition / Cope elimination sequence was developed, which constructed the core with a heteroaryl- substituted triazole in place in a single step. This novel method is expected to have utility in the rapid construction of a broader class of fused triazole systems.

Besides having high aqueous solubility, compound **35** showed an increased plasma free fraction compared to closely related fused 1,2,3-triazole core compounds. This is also thought to be due to the isonicotinamide moiety. Compound **35** showed excellent P2X7 receptor occupancy in the hippocampus of rats, demonstrating a low ED_{50} of 0.07 mg/kg and unbound plasma EC_{50} of 12 ng/mL. In addition, **35** suppressed brain IL-1β release in vivo in freely moving rats challenged with the P2X7 agonist Bz-ATP. The compound also demonstrated good tolerability margins in preclinical species, as well as an acceptable cardiovascular safety profile in vivo. FIH enabling safety studies are currently underway for compound **35** in anticipation of Phase I clinical trials to determine the safety and tolerability of **35** in healthy human subjects.

EXPERIMENTAL SECTION:

Solvents and reagents were used as supplied by the manufacturer. Concentrated refers to concentrated using a rotary evaporator under reduced pressure.

Unless specified otherwise, normal-phase silica gel column chromatography was performed on silica gel (SiO_2) using prepackaged cartridges and the indicated solvents. Preparative reverse-phase high performance liquid chromatography (HPLC) was performed on an Agilent HPLC with a Waters XBridge C18 column or Xterra Prep RP_{18} column (5 μm, 30x100 mm or 50x150 mm) and a gradient of 5-99% acetonitrile/water (20 mM NH_4OH) over 12 to 18 min and a flow rate of 30 or 80 ml/min, unless otherwise indicated. Preparative SFC was performed either on a JASCO preparative SFC system, an APS 1010 system from Berger instruments, or an SFC-

PICLAB-PREP 200 (PIC SOLUTION, Avignon, France). The separations were conducted between 100-150 bar with a flow rate ranging from 40-60 mL/min. The columns used were heated to 35-40 °C.

Mass spectra were obtained on an Agilent series 1100 MSD using electrospray ionization (ESI) in positive mode. The calculated (calcd) mass corresponds to the exact mass. HRMS was obtained on a Bruker microTOF, using ESI in positive mode with a scan range of 200-700 amu. Sodium formate solution (Fluka 97574-100mL) was used to calibrate the TOF and as an internal standard. High accuracy MS was run on an Agilent 5975 Series GCMS; EI source. Cerno Biosciences Mass works software was used to process the data. PFTBA was used as an internal calibrant. Nuclear magnetic resonance (NMR) spectra were obtained on Bruker model DRX spectrometers. If rotamers were present, VT NMR was used to determine which peaks coalesce at 120 °C in *d*-DMSO. The ^{1}H spectra are reported as a mixture of all rotamers at rt in *d*-$CDCl_3$ or *d*-DMSO and the ^{13}C are reported as the major rotamer only at rt in *d*-DMSO.

Melting points (mp) were determined using differential scanning calorimetry (DSC) on a TA Instruments™ Q200 series instrument equipped with a standard cell (FC). The DSC was cooled using a TA Instruments Refrigerated Cooling System 90 (RCS 90). Nitrogen gas purge was set to 50 mL/min. The DSC method equilibrated at 25°C and used a heating ramp of 10°C/min up to 300°C. Samples were analyzed in pinhole hermetic pans. Data analysis was performed using TA Universal Analysis software. Data is reported as the range of T_{onset} - T_{peak}.

All compounds tested were of a minimum of 95% purity as determined by HPLC. The HPLC method used for purity determinations is as follows: Analytical LCMS was obtained on an Agilent 1100/1200 series LCMS with ESI in positive mode and a scan range of 100-700 amu. Samples were run on a Halo C18 column (2.7um, 50 x 3 mm), with a mobile phase of 5-99%

ACN in 0.05% TFA over 3.5 min and then hold at 99% ACN for 0.5 min, at a flow rate of 1 mL/min (Temperature = 50 °C).

Two-step cycloaddition / Cope elimination procedure A. *Step 1. tert-Butyl (S)-6-methyl-1-phenyl-7a-(pyrrolidin-1-yl)-1,3a,4,6,7,7a-hexahydro-5H-[1,2,3]triazolo[4,5-c]pyridine-5-carboxylate (**7a**)* and *tert-Butyl (4S)-4-methyl-1-phenyl-7a-(pyrrolidin-1-yl)-1,3a,4,6,7,7a-hexahydro-5H-[1,2,3]triazolo[4,5-c]pyridine-5-carboxylate (**8a**)*. To a solution of *rac*-**6** (210 mg, 0.98 mmol) in toluene (5 mL) at 100 °C in a sealed tube was added, phenyl azide (152 mg, 1.28 mmol) followed immediately by pyrrolidine (0.08 mL, 0.98 mmol). The reaction was stirred for 75 min at 100 °C and became dark red in color. It was cooled to rt and a solution of sat. $NaHCO_3$ (5 mL) was added. After stirring for 30 min the layers were separated and the water layer was extracted once with EtOAc. The organic layers were combined, dried over $MgSO_4$, and concentrated. The residue was purified by flash chromatography (SiO_2; 0-30% EtOAc /hexanes) to give the title compounds (119 mg, 31% for the first eluting peak, **8a**; 121 mg, 32% for the second eluting peak, **7a**). MS (ESI) mass calcd. $C_{21}H_{31}N_5O_2$, 385.2 for **7a**; m/z found, 386.1 $[M+H]^+$. ^1H NMR of **7a** (400 MHz, $CDCl_3$) δ 7.68 – 7.46 (m, 2H), 7.42 – 7.29 (m, 2H), 7.17 – 7.04 (m, 1H), 4.64 – 4.33 (m, 2H), 3.68 – 3.00 (br m, 2H), 2.63 – 2.35 (m, 5H), 2.02 – 1.89 (m, 1H), 1.82 – 1.67 (m, 4H), 1.58 – 1.35 (m, 9H), 1.03 (d, *J* = 5.7 Hz, 3H). MS (ESI) mass calcd. $C_{21}H_{31}N_5O_2$, 385.2 for **8a**; m/z found, 386.1 $[M+H]^+$. ^1H NMR of **8a** (500 MHz, $CDCl_3$) δ 7.71 – 7.61 (m, 2H), 7.39 – 7.28 (m, 2H), 7.16 – 7.07 (m, 1H), 4.73 (br s, 1H), 4.27 (s, 1H), 3.37 – 3.24 (m, 1H), 2.84 – 2.71 (m, 1H), 2.65 – 2.51 (m, 4H), 2.43 – 2.26 (m, 2H), 1.87 – 1.74 (m, 4H), 1.59 – 1.35 (m, 12H).

*Step 2. tert-Butyl 4-methyl-1-phenyl-1,4,6,7-tetrahydro-5H-[1,2,3]triazolo[4,5-c]pyridine-5-carboxylate (**9a**).* To a solution of **7a** (120 mg, 0.31 mmol) in DCM (3 mL) was added $NaHCO_3$

(25 mg, 0.31 mmol) and *m*-CPBA (103 mg, 0.46 mmol). The reaction was stirred for 5 min then 0.6N $NaHSO_3$ (3 mL) was added. After stirring for 30 min the layers were separated and the water layer was extracted two times more with DCM. The organic layers were combined, dried over $MgSO_4$, and concentrated. The residue was purified by flash chromatography (SiO_2; 0-100% EtOAc/hexanes) to give the title compound (81 mg, 83%). MS (ESI) mass calcd. $C_{17}H_{22}N_4O_2$, 314.1; m/z found, 315.1 $[M+H]^+$. ^1H NMR (400 MHz, $CDCl_3$) δ 7.72 – 7.50 (m, 5H), 4.93 (d, *J* = 16.3 Hz, 1H), 4.82-4.72 (m, 1H), 4.18 (d, *J* = 15.9 Hz, 1H), 3.30 – 3.19 (m, 1H), 2.65 – 2.57 (m, 1H), 1.45 (s, 9H), 1.02 (d, *J* = 6.9 Hz, 3H).

Synthesis of 2-azido-5-fluoropyrimidine. Safety Note: Extreme caution should be exercised when synthesizing/using organic azides. Organic azides are especially sensitive to violent decomposition from external energy sources such as light, heat, friction, and pressure. The stability of an organic azide is dependent upon its chemical structure. 2-Azido-5-fluoropyrimidine underwent thermal and shock sensitivity analysis before isolating quantities > 1g. See Supplementary information for more details.

Step 1. 5-Fluoro-2-hydrizinylpyrimidine. To a solution of 2-chloro-5-fluoropyrimidine (0.983 g, 7.42 mmol) in EtOH (10 mL) was added hydrazine monohydrate (0.233 mL, 7.42 mmol). The flask was stirred at reflux for 16 h. The reaction was cooled and evaporated under reduced pressure and MeOH was added until the solids dissolved. Silica gel was added (10 g) and the solids were concentrated to dryness. The compound was purified by flash chromatography (0-6% 2N NH_3 in MeOH/DCM gradient over 20 min) to yield the product as a white solid (0.74 g, 78%). ^1H NMR (400 MHz, DMSO-d_6) δ 8.40 (d, *J* = 1.0 Hz, 2H), 8.19 (s, 1H), 4.13 (s, 2H).

Step 2. 2-Azido-5-fluoropyrimidine. To a solution of 5-fluoro-2-hydrizinylpyrimidine (3.19 g, 24.9 mmol) in 3:1 acetic acid/water (100 mL) at 5 °C was added dropwise over 30 min by

addition funnel a solution of sodium nitrite (3.44 g, 49.8 mmol) in water (25 mL). After completion of addition, the reaction was stirred for 2 h at 5 °C, and then diluted with more water (100 mL). The solution was extracted with Et_2O/pentane (1:1) (3x100 mL). The organic layers were combined and made basic to pH 8 using sat Na_2CO_3 (~500 mL) and stirring. The layers were separated and the water layer was extracted three times more with Et_2O/pentane. The organic layers were combined, washed with brine, dried with $MgSO_4$, filtered and evaporated under reduced pressure over an ice bath to give a white solid at 0 °C (2.92 g, 84%) which melted upon warming to rt. ^{1}H NMR (600 MHz, $CDCl_3$) δ 8.47 (s, 1H). ^{13}C NMR (151 MHz, $CDCl_3$) δ 158.13, 158.12, 156.01, 154.29, 146.91, 146.76. GCMS (EI) mass calc. for $C_4H_2N_5F$, 139.0289; m/z found 139.0314 (spectral accuracy = 97.43%).

One-pot cycloaddition / Cope elimination procedure B. *tert-Butyl (S)-1-(5-fluoropyrimidin-2-yl)-6-methyl-1,4,6,7-tetrahydro-5H-[1,2,3]triazolo[4,5-c]pyridine-5-carboxylate (**9b**)* and *tert-butyl (S)-1-(5-fluoropyrimidin-2-yl)-4-methyl-1,4,6,7-tetrahydro-5H-[1,2,3]triazolo[4,5-c]pyridine-5-carboxylate (**10b**)*. To a solution of **(S)-6** (2.76 g, 12.9 mmol) in toluene (100 mL) at 100 °C was added 2-azido-5-fluoropyrimidine (2.34 g, 16.8 mmol) as a solution in toluene (15 mL) followed by pyrrolidine (1.06 mL, 12.9 mmol). After stirring for 3 h, the reaction was cooled to 0 °C and CH_2Cl_2 (100 mL) was added followed by $NaHCO_3$ (2.17g, 25.9 mmol) and *m*-CPBA (4.47g, 25.9 mmol). The reaction was allowed to warm to rt over 30 min followed by the addition of 1N NaOH (100 mL). The organic layer was separated and the water layer was extracted with CH_2Cl_2 two times. The combined organic layers were dried over anhydrous $MgSO_4$, filtered and concentrated. Chromatography on silica gel (0-100% ethyl acetate/hexanes) provided the desired product as a mixture of regioisomers. ^{1}H NMR integration of the C6-methyl group was used to determine the ratio of products (9:1 = **9b**: **10b**, 2.85g, 66%). MS (ESI) mass

calcd. $C_{15}H_{19}FN_6O_2$, 334.16; m/z found, 335.2 $[M+H]^+$. ^1H NMR of major regioisomer (500 MHz, $CDCl_3$) δ 8.73 (s, 2H), 5.16 (d, *J* = 16.1 Hz, 1H), 4.96 (br s, 1H), 4.25 (d, *J* = 16.4 Hz, 1H), 3.38 – 3.28 (m, 1H), 3.19 – 3.10 (m, 1H), 1.50 (s, 9H), 1.16 (d, *J* = 7.0 Hz, 3H).

General procedure for the preparation of 1-aryl substituted triazoles (Compounds 11-20). To a solution of the ketone (0.5 mmol) in toluene (2.5 mL) under N_2 at 100 ^{0}C was added the aryl azide (1.0 mmol) followed by pyrrolidine (0.5 mmol). After stirring at 100 ^{0}C for 2h the reaction was cooled to room temperature, uncapped, and diluted with DCM (2 mL). *m*-CPBA (0.75 mmol) and $NaHCO_3$ (1.0 mmol) were added and allowed to stir for 30 minutes. Saturated $NaHCO_3$ (2.5 ml) was added and allowed to stir for an additional 30 minutes. The organic phase was separated, and the aqueous phase was washed 2x with DCM. The organic layers were combined, dried over $MgSO_4$, and concentrated. The crude product was purified by column chromatography (0-50% EtOAc/Hex), to afford the triazole product.

tert-Butyl 1-phenyl-1,4,6,7-tetrahydro-5H-[1,2,3]triazolo[4,5-c]pyridine-5-carboxylate ***(11)***. Isolated as a light yellow solid (66%). Mp 133.97-136.12 °C. ^1H NMR (400 MHz, $CDCl_3$) δ 7.57-7.52 (m, 4H), 7.50-7.45 (m, 1H), 4.73 (s, 2H), 3.76 (s, 2H), 2.87 (t, *J*=5.58 Hz, 2H), 1.50 (s, 9H). ^{13}C NMR (100 MHz, $CDCl_3$) δ 155.01, 141.81, 136.49, 130.90, 129.78, 129.08, 122.93, 80.74, 41.94, 40.45, 28.50, 22.47. HRMS calc. for $C_{16}H_{20}N_4O_2$ $[M+H]^+$ 301.1659, found 301.1669.

1-Phenyl-4,5,6,7-tetrahydro-1H-benzo[d][1,2,3]triazole ***(12)***. Isolated as a light yellow solid (59%). Mp 116.46-117.40 °C. ^1H NMR (400, MHz, $CDCl_3$) δ 7.56-7.49 (m, 4H) 7.44 (m, 1H) 2.84 (t, *J*=5.00 Hz, 2H), 2.74 (t, *J*=4.99 Hz, 2H), 1.91-1.84 (m, 4H). ^{13}C NMR (100 MHz, $CDCl_3$) δ 144.11, 137.05, 132.21, 129.61, 128.76, 123.29, 22.91, 22.63, 22.10, 22.00. HRMS calc. for $C_{12}H_{13}N_3$ $[M+H]^+$ 200.1182, found 200.1198.

*tert-Butyl 1-phenyl-4,5,7,8-tetrahydro-[1,2,3]triazolo[4,5-d]azepine-6(1H)-carboxylate (**13a**)*. Isolated as the first of two peaks after chromatographic separation as a white solid (31%). Mp 153.60-157.26 °C. ^{1}H NMR (400, MHz, $CDCl_3$) δ 7.52 (m, 3H), 7.43-7.41 (m, 2H), 3.65-3.57 (m, 4H), 3.18-3.12 (m, 2H), 2.92-2.80 (m, 2H), 1.50 (s, 9H). ^{13}C NMR (100 MHz, $CDCl_3$) δ 154.72, 144.86, 136.62, 133.99, 129.48, 125.33, 125.25, 80.21, 47.93, 46.71, 28.51, 27.88, 25.21. HRMS calc. for $C_{17}H_{22}N_4O_2$ $[M+H]^+$ 315.1816, found 315.1830.

*tert-Butyl 1-phenyl-4,6,7,8-tetrahydro-[1,2,3]triazolo[4,5-c]azepine-5(1H)-carboxylate (**13b**)*. Isolated as the second of two peaks after chromatographic separation as a white solid (32%). Mp 110.57-113.20 °C. ^{1}H NMR (400, MHz, $CDCl_3$) δ 7.56-7.50 (m, 3H), 7.44-7.41 (m, 2H), 4.80-4.74 (m, 2H), 3.72-3.64 (m, 2H), 2.82 (t, *J*=6.07 Hz, 2H), 1.93 (s, 1H) 1.45(s, 9H). ^{13}C NMR (100 MHz, $CDCl_3$) δ 155.03, 145.18, 136.23, 134.89, 129.48, 125.17, 80.33, 48.45, 44.46, 28.39, 26.14, 23.22. HRMS calc. for $C_{17}H_{22}N_4O_2$ $[M+H]^+$ 315.1816, found 315.1822.

*1-Phenyl-1,4,6,7-tetrahydropyrano[3,4-d][1,2,3]triazole (**15**)*. Isolated as a light yellow solid (25%). Mp 92.94-94.65 °C. ^{1}H NMR (400, MHz, $CDCl_3$) δ 7.60-7.53 (m, 4H), 7.47 (m, 1H), 4.91 (t, *J* =1.28 Hz, 2H), 3.97 (t, *J*=5.47 Hz, 2H), 2.93 (tt, *J*=5.43 Hz, 1.27 Hz, 2H). ^{13}C NMR (100 MHz, $CDCl_3$) δ 142.39, 136.62, 129.84, 129.64, 129.08, 122.84, 64.23, 64.10, 23.61. HRMS calc. for $C_{11}H_{11}N_3O$ $[M+H]^+$ 202.0975, found 202.0980.

*1-Phenyl-1,4,6,7-tetrahydrothiopyrano[3,4-d][1,2,3]triazole (**16**)*. Isolated as a yellow amorphous solid (8%). ^{1}H NMR (400, MHz, $CDCl_3$) δ 7.57-7.48 (m, 5H), 3.95 (s, 2H), 3.01 (t, *J*=5.52 Hz, 2H), 2.91 (t, *J*=5.70 Hz, 2H). ^{13}C NMR (100 MHz, $CDCl_3$) δ 139.98, 136.62, 131.88, 129.61, 129.21, 123.88, 25.65, 24.57, 23.50. HRMS calc. for $C_{11}H_{11}N_3S$ $[M+H]^+$ 218.0746, found 208.0755.

*tert-Butyl 1-benzyl-1,4,6,7-tetrahydro-5H-[1,2,3]triazolo[4,5-c]pyridine-5-carboxylate (**18**).* Isolated as a white solid (38%). Mp 131.43-133.23 °C. ^{1}H NMR (400, MHz, $CDCl_3$) δ 7.37-7.32 (m, 3H), 7.21-7.19 (m, 2H), 5.46 (s, 2H), 4.62 (s, 2H), 3.65 (s, 2H), 2.51 (s, 2H), 1.45 (s, 9H). ^{13}C NMR (100 MHz, $CDCl_3$) δ 154.93, 141.73, 134.51, 130.89, 129.22, 128.70, 127.75, 80.67, 52.32, 41.92, 40.26, 28.49, 20.93. HRMS calc. for $C_{14}H_{24}N_4O_2$ $[M+H]^+$ 281.1972, found 281.1967.

*tert-Butyl 1-(4-fluorophenyl)-1,4,6,7-tetrahydro-5H-[1,2,3]triazolo[4,5-c]pyridine-5-carboxylate (**19**).* Isolated as a light yellow solid (32% and 50% for n=2 reactions). Mp 127.95-129.74 °C. ^{1}H NMR (400, MHz, $CDCl_3$) δ 7.55-7.51 (m, 2H), 7.22 (m, 2H), 4.72 (s, 2H), 3.76 (s, 2H), 2.83 (t, *J*=5.56, 2H), 1.50 (s, 9H). ^{13}C NMR (100 MHz, $CDCl_3$) δ 163.54, 161.55, 154.87, 141.76, 132.52, 124.85, 124.78, 116.80, 116.62, 80.68, 41.74, 40.33, 28.37, 22.23. HRMS calc. for $C_{16}H_{19}N_4O_2F$ $[M+H]^+$ 319.1565, found 319.1570.

*tert-Butyl 1-(4-methoxyphenyl)-1,4,6,7-tetrahydro-5H-[1,2,3]triazolo[4,5-c]pyridine-5-carboxylate (**20**).* Isolated as an orange oil (13%). ^{1}H NMR (400, MHz, $CDCl_3$) δ 7.46-7.43 (m, 2H), 7.04-7.02 (m, 2H), 4.72 (s, 2H), 3.87 (s, 3H), 3.75 (s, 2H), 2.81 (t, *J*=5.56, 2H), 1.50 (s, 9H). ^{13}C NMR (100 MHz, $CDCl_3$) δ 160.11, 155.08, 141.55, 129.56, 124.58, 114.90, 114.36, 80.75, 55.77, 42.12, 40.45, 28.53, 22.28. HRMS calc. for $C_{17}H_{22}N_4O_3$ $[M+H]^+$ 331.1765, found 331.1619.

General procedure for the preparation of 1-alkyl substituted triazoles (Compounds 21-25). The procedure using alkyl azides is the same as the general procedure for aryl azides except the reaction was heated for 18 h at 100 °C.

*tert-Butyl 1-isopropyl-1,4,6,7-tetrahydro-5H-[1,2,3]triazolo[4,5-c]pyridine-5-carboxylate (**21**).* Isolated as a yellow oil (55%). ^{1}H NMR (400, MHz, $CDCl_3$) δ 4.63 (m, 3H)*, 3.75 (m, 2H), 2.74

(t, *J*=5.60 Hz, 2H), 1.59 (d, *J*=6.79, 6H), 1.48 (s, 9H). ^{13}C NMR (100 MHz, $CDCl_3$) δ 155.00, 141.19, 129.59, 80.62, 51.54, 42.05, 40.37, 28.50, 22.49, 21.24

*Overlapped alkyl singlet from piperdine ring with the septet of isopropyl proton. HRMS calc. for $C_{13}H_{22}N_4O_2$ $[M+H]^+$ 267.1816, found 267.1819.

*tert-Butyl 1-isopropyl-4,5,6,7-tetrahydro-1H-benzo[d][1,2,3]triazole (**22**).* Isolated as a yellow oil (38%). ^{1}H NMR (400, MHz, $CDCl_3$) δ 4.55 (sept, *J*=6.78, 1H), 2.75 (t, *J*=6.0 Hz, 2H), 2.62 (t, *J*=6.0 Hz, 2H), 1.83 (m, 4H), 1.57 (d, *J*=6.78, 6H). ^{13}C NMR (100 MHz, $CDCl_3$) δ 143.48, 130.77, 51.01, 22.88, 22.75, 22.47, 22.10, 20.59. HRMS calc. for $C_9H_{15}N_3$ $[M+H]^+$ 166.1339, found 166.1339.

*tert-Butyl 1-isopropyl-4,5,7,8-tetrahydro-[1,2,3]triazolo[4,5-d]azepine-6(1H)-carboxylate (**23a**) and tert-Butyl 1-isopropyl-4,6,7,8-tetrahydro-[1,2,3]triazolo[4,5-c]azepine-5(1H)-carboxylate (**23b**).* Two products isolated together as a colorless oil (43%). ^{1}H NMR (400 MHz, $CDCl_3$) δ 4.76-4.60 (m, 2H), 4.56-4.44 (m, 2H), 3.73-3.55 (m, 4H), 2.90-2.75 (m, 4H), 2.91 – 2.74 (m, 4H), 2.03-1.92 (m, 2H), 1.58 (d, *J* = 6.7 Hz, 12H), 1.50-1.37 (br m, 18H). MS (ESI): mass calc. for $C_{14}H_{24}N_4O_2$, 280.19; found 281.1 $[M+H]^+$.

*tert-Butyl 1-isopropyl-1,4,6,7-tetrahydrothiopyrano[3,4-d][1,2,3]triazole (**25**).* Isolated as an oily solid (13-24%). ^{1}H NMR (400, MHz, $CDCl_3$) δ 4.52 (sept, *J*=6.73 Hz, 1H), 3.85 (s, 2H), 2.93 (m, 4H), 1.60 (d, *J*=6.75 Hz, 6H). ^{13}C NMR (100 MHz, $CDCl_3$) δ 139.50, 130.24, 50.95, 25.59, 23.64, 23.19, 22.36. HRMS calc. for $C_8H_{13}N_3S$ $[M+H]^+$ 184.0903, found 184.0908.

*(S)-(2-Chloro-3-(trifluoromethyl)phenyl)(6-methyl-1-phenyl-1,4,6,7-tetrahydro-5H-[1,2,3]triazolo[4,5-c]pyridin-5-yl)methanone (**26**). Step 1.* To a solution of **(S)-9a** obtained from Two-Step Procedure A (170 mg, 0.54 mmol) in CH_2Cl_2 (10 mL) was added 2M HCl in diethyl ether (1.4 mL, 2.7 mmol). After stirring overnight at rt, the reaction was concentrated to give (S)-

6-methyl-1-phenyl-4,5,6,7-tetrahydro-1H-[1,2,3]triazolo[4,5-c]pyridine as a light yellow solid (135 mg, 100%), and used directly in the next reaction. MS (ESI) mass calcd. $C_{12}H_{14}N_4$, 214.1; m/z found, 215.3 $[M+H]^+$.

Step 2. **General amide coupling conditions.** To a solution of (*S*)-6-methyl-1-phenyl-4,5,6,7-tetrahydro-1*H*-[1,2,3]triazolo[4,5-*c*]pyridine (180 mg, 0.77 mmol) in CH_2Cl_2 (6 mL) in triethylamine (0.3 mL, 2.3 mmol) was added 2-chloro-3-(trifluoromethyl)benzoyl chloride. After stirring for 15 min at rt, aq sodium bicarbonate was added (2 mL). The water layer was separated and extracted 2x with CH_2Cl_2. The organic layers were combined, dried (Na_2SO_4) and concentrated. The residue was purified by flash chromatography (0-100% EtOAc/hexane over 15 min, 40g column, 40 mL/min). The product was isolated as a colorless oil (172 mg, 76%). ^{1}H NMR (400 MHz, $CDCl_3$) δ 7.83 – 7.76 (m, 1H), 7.60 – 7.43 (m, 7H), 5.84 (dd, *J* = 16.9, 11.0 Hz, 0.5H), 5.71 – 5.63 (m, 0.5H), 4.66 – 4.34 (m, 1.5H), 4.12 – 4.06 (m, 0.75H), 3.41 – 3.26 (m, 0.75H), 3.06 - 2.98 (m, 0.15H), 2.77 – 2.52 (m, 0.85H), 1.34 – 1.13 (m, 3H). MS (ESI) mass calcd. $C_{20}H_{16}ClF_3N_4O$, 420.1037; m/z found, 421.1041 $[M+H]^+$.

*(S)-(2-Chloro-3-(trifluoromethyl)phenyl)(1-(5-fluoropyrimidin-2-yl)-6-methyl-1,4,6,7-tetrahydro-5H-[1,2,3]triazolo[4,5-c]pyridin-5-yl)methanone (**27**). Step 1. (S)-1-(5-Fluoropyrimidin-2-yl)-6-methyl-4,5,6,7-tetrahydro-1H-[1,2,3]triazolo[4,5-c]pyridine (**41**)*. To a solution of **(S)-9b+10b** obtained from One-Pot Procedure B (9:1, 8.33 g, 24.9 mmol) in CH_2Cl_2 (125 mL) was added 4M HCl in 1,4-dioxane (31 mL, 125 mmol). After stirring for 4h, MeOH was added until the oils dissolved. The reaction stirred at rt for 3d after which the solvents were evaporated in vacuo. The residue was stirred in CH_2Cl_2 (200 mL) and sat sodium bicarbonate (200 mL) for 1h. The layers were separated and the water layer was extracted 2x with CH_2Cl_2. The organic layers were combined, dried ($MgSO_4$), filtered and concentrated. The residue was

stirred in EtOAc (25 mL) at 40 °C overnight. The solids were collected by suction filtration to give pure **41** (1.3 g, 22%). The filtrate was concentrated and purified by prep HPLC (Agilent, Waters XBridge C18 5μm 50x100 mm column, 5-60% MeCN/20 mM NH_4OH over 13 min, 80 mL/min) to give to second crop of **41** (1.9 g, 31%) and isolate **42** (300 mg, 5%). ^{1}H NMR (400 MHz, DMSO) δ 9.97 – 9.69 (m, 1H), 9.15 (s, 2H), 4.58 – 4.35 (m, 2H), 3.80 – 3.47 (m, 2H), 3.21 – 3.03 (m, 1H), 1.46 (d, *J* = 6.5 Hz, 3H). MS (ESI) mass calcd. $C_{10}H_{11}FN_6$, 234.23; m/z found, 235.1 $[M+H]^+$. ^{13}C NMR (151 MHz, $CDCl_3$) δ 157.42, 155.67, 151.57, 151.55, 146.82, 146.67, 143.73, 132.90, 76.84, 48.95, 42.11, 32.80, 21.66. ^{1}H NMR of **27** (600 MHz, $CDCl_3$) δ 8.72 (s, 2H), 4.24 – 4.17 (m, 1H), 3.41 – 3.34 (m, 1H), 3.19 – 3.10 (m, 2H), 3.06 – 2.98 (m, 1H), 1.58 (d, *J* = 6.7 Hz, 3H). MS (ESI) mass calcd. $C_{10}H_{11}FN_6$, 234.23; m/z found, 235.1 $[M+H]^+$. ^{13}C NMR (151 MHz, $CDCl_3$) δ 157.43, 155.68, 151.64 (d, *J* = 3.5 Hz), 147.97, 146.83, 146.68, 132.08, 77.03, 76.81, 48.20, 41.69, 25.77, 20.16.

Step 2. Conducted using the general amide coupling conditions (192 mg, 57%). ^{1}H NMR (500 MHz, $CDCl_3$) δ 8.81 – 8.69 (m, 2H), 7.82 – 7.74 (m, 1H), 7.59 – 7.40 (m, 2H), 5.90 – 5.79 (m, 0.5H), 5.71 – 5.60 (m, 0.5H), 4.68 – 4.31 (m, 1.5H), 4.12 – 4.06 (m, 0.5H), 3.57 – 3.07 (m, 2H), 1.39 – 1.31 (m, 3H). MS (ESI) mass calcd. $C_{18}H_{13}ClF_4N_6O$, 440.0848; m/z found, 441.0861 $[M+H]^+$.

Compounds **28,29,35-38** were prepared from intermediate **41** using the General amide coupling conditions.

Compounds **32-34**, **39-40** were synthesized using One-pot cycloaddition / Cope elimination Procedure B followed by Boc-deptrotection as described for **26** and General amide coupling conditions. Compounds **30-31** were synthesized using the former route employed prior to this methodology development. It is described in the supporting information.

Compounds **28-40** were isolated as a mixture of several rotamers. The NMR spectra are reported as a mixture of several rotamers. In most cases obtaining ^{13}C spectra required highly concentrated samples and resulted in > 40 peaks. As such, ^{13}C data is generally not reported.

For compounds **35-40,** melting points are not given; these compounds were found to be amorphous by DSC and did not melt, or resulted in a gradual melt with decomposition (30-300 °C).

*(S)-1-(5-Fluoropyrimidin-2-yl)-6-methyl-5-{[2-methyl-3-(trifluoromethyl)phenyl]carbonyl}-4,5,6,7-tetrahydro-1H-[1,2,3]triazolo[4,5-c]pyridine (**28**)*. Isolated as a white solid (98 mg, 52%). Mp 224.27-225.75 °C. ^1H NMR (400 MHz, $CDCl_3$) δ 8.79 – 8.70 (m, 2H), 7.75 – 7.67 (m, 1H), 7.46 – 7.27 (m, 2H), 5.93 – 5.81 (m, 0.5H), 5.75 – 5.62 (m, 0.5H), 4.60 – 4.30 (m, 1.5H), 4.20 – 4.08 (m, 0.5H), 3.55 – 3.04 (m, 2H), 2.55 – 2.20 (m, 3H), 1.40 – 1.15 (m, 3H). MS (ESI) mass calcd. for $C_{19}H_{16}F_4N_6O$ $[M+H]^+$, 421.1394; m/z found, 421.1403 $[M+H]^+$.

*(S)-1-(5-Fluoropyrimidin-2-yl)-5-{[2-fluoro-3-(trifluoromethyl)phenyl]carbonyl}-6-methyl-4,5,6,7-tetrahydro-1H-[1,2,3]triazolo[4,5-c]pyridine (**29**)*. Method I. To a solution of **41** (213 mg, 0.91 mmol), Hunig's base (0.3 mL, 1.8 mmol), 2-fluoro-3-(trifluoromethyl)benzoic acid (227 mg, 1.09 mmol) in CH_2Cl_2 (10 mL) was added 2,4,6-Tripropyl-1,3,5,2,4,6-trioxatriphosphorinane-2,4,6-trioxide (50% solution in CH_2Cl_2). The reaction stirred for 3d then water (10 mL) was added. The layers were separated and the organic layer was dried ($MgSO_4$). Flash chromatography (0-10% (2 NH_3 in MeOH)/CH_2Cl_2 gradient) provided the title compound as a white solid (238 mg, 62%). Mp 218.97-219.88 °C. HPLC t_R = 9.478 (Stationary phase: CHIRALPAK AD-H 5µm 250 x 4.6mm), Mobile phase: 90% CO_2, 10% EtOH). Method II. To a 9:1 mixture of **41:42** (7.97 g, 29.4 mmol) and triethylamine (16 mL, 118 mmol) in CH_2Cl_2 at 0 °C was added 2-fluoro-3-(trifluoromethyl)benzoyl chloride. After stirring for 2 h sat $NaHCO_3$

(200 mL) was added. The layers were separated and the water layer was extracted 2x with CH_2Cl_2. The organic layers were combined and dried ($MgSO_4$). The crude material was evaporated to dryness. MeOH (80 mL) was added and the slurry was sonicated and then stirred at 60 °C for 4h. The solids were collected by suction filtration and allowed to air dry overnight (5.5 g, 44%). Mp 216.79-218.55 °C. ^{1}H NMR (500 MHz, $CDCl_3$) δ 8.79 – 8.68 (m, 2H), 7.79 – 7.54 (m, 2H), 7.46 – 7.30 (m, 1H), 5.97 – 5.55 (m, 1H), 4.77 – 4.19 (m, 2H), 3.58 – 3.11 (m, 2H), 1.43 – 1.14 (m, 3H). MS (ESI) mass calcd. $C_{18}H_{13}F_5N_6O$, 424.1; m/z found, 424.8 $[M+H]^+$. HPLC t_R = 9.478 (Stationary phase: CHIRALPAK AD-H 5µm 250 x 4.6mm), Mobile phase: 90% CO_2, 10% EtOH). The filtrate was concentrated and purified by SFC (Stationary phase: diethylaminopropyl 5µm 150x21.2mm), Mobile phase: 95% CO_2, 5% MeOH) (3.1 g, 65%). Mp 218.51-220.00 °C. Rotamer peaks were found to coalesce at 120 °C in d-DMSO, these data are reported for **29**: ^{1}H NMR (600 MHz, DMSO, 120 °C) δ 9.02 – 8.98 (s, 2H), 7.87 – 7.82 (m, 1H), 7.80 – 7.74 (m, 1H), 7.53 – 7.48 (m, 1H), 5.53 – 4.81 (m, 1H), 4.45 – 4.33 (d, *J* = 15.9 Hz, 1H), 3.30 – 3.20 (s, 1H), 3.18 – 3.09 (m, 1H), 1.58 – 1.44 (m, 1H), 1.23 – 1.14 (d, *J* = 6.9 Hz, 3H). ^{13}C NMR (151 MHz, DMSO, 120 °C) δ 163.49, 157.73, 155.99, 150.92, 150.89, 147.33, 147.18, 138.94, 133.21, 133.18, 130.73, 128.38, 128.35, 126.25, 126.13, 125.63, 125.60, 123.33, 121.53, 117.70, 117.62, 117.48, 117.40, 29.11, 17.43. MS (ESI) mass calcd. for $C_{18}H_{13}F_5N_6O$ $[M+H]^+$, 425.1144; m/z found, 425.1145 $[M+H]^+$. HPLC t_R = 9.480 (Stationary phase: CHIRALPAK AD-H 5µm 250 x 4.6mm), Mobile phase: 90% CO_2, 10% EtOH). Specific rotation: $[\alpha]^{20}{}_D$ +34.3 (c 0.452, CH_3OH).

(S)-(2-chloro-3-(trifluoromethyl)phenyl)(6-methyl-1-(pyridin-2-yl)-1,4,6,7-tetrahydro-5H-[1,2,3]triazolo[4,5-c]pyridin-5-yl)methanone (**30**).* ^{1}H NMR (400 MHz, $CDCl_3$) δ 8.56 – 8.41 (m, 1H), 8.23 – 8.12 (m, 1H), 7.98 – 7.89 (m, 1H), 7.82 – 7.74 (m, 1H), 7.57 – 7.30 (m, 3H),

5.90 – 5.78 (m, 0.5H), 5.70 – 5.59 (m, 0.5H), 4.67 – 4.31 (m, 1.5H), 4.14 – 4.01 (m, 0.5H), 3.59 – 3.20 (m, 2H), 1.39 – 1.30 (m, 2.3H), 1.20 (d, J = 6.8 Hz, 0.7H). MS (ESI) mass calcd. for $C_{19}H_{15}ClF_3N_5O$ $[M+H]^+$, 422.0990; m/z found, 422.1004 $[M+H]^+$.

(S)-(2-chloro-3-(trifluoromethyl)phenyl)(6-methyl-1-(pyrazin-2-yl)-1,4,6,7-tetrahydro-5H-[1,2,3]triazolo[4,5-c]pyridin-5-yl)methanone (**31**).* ^{1}H NMR (500 MHz, $CDCl_3$) δ 9.57 – 9.49 (m, 1H), 8.69 – 8.63 (m, 1H), 8.52 – 8.48 (m, 0.5H), 8.45 – 8.38 (m, 0.5H), 7.82 – 7.76 (m, 1H), 7.58 – 7.39 (m, 2H), 5.91 – 5.81 (m, 0.5H), 5.71 – 5.61 (m, 0.5H), 4.67 – 4.32 (m, 1.5H), 4.14 – 4.04 (m, 0.5H), 3.58 – 3.11 (m, 2H), 1.40 – 1.31 (m, 2.3H), 1.23 – 1.19 (m, 0.7H). MS (ESI) mass calcd. for $C_{18}H_{14}ClF_3N_6O$ $[M+H]^+$, 423.0942; m/z found, 423.0948 $[M+H]^+$.

*(S)-(2-Chloro-3-(trifluoromethyl)phenyl)(1-(1-ethyl-1H-pyrazol-3-yl)-6-methyl-6,7-dihydro-1H-[1,2,3]triazolo[4,5-c]pyridin-5(4H)-yl)methanone (**32**).*

Step 1. General procedure B was used to give intermediates *tert*-butyl (*S*)-1-(1-ethyl-1*H*-pyrazol-3-yl)-6-methyl-1,4,6,7-tetrahydro-5*H*-[1,2,3]triazolo[4,5-*c*]pyridine-5-carboxylate and *tert*-butyl (*S*)-1-(1-ethyl-1H-pyrazol-3-yl)-4-methyl-1,4,6,7-tetrahydro-5*H*-[1,2,3]triazolo[4,5-*c*]pyridine-5-carboxylate (284 mg, 60%, 1:1). ^{1}H NMR (500 MHz, $CDCl_3$) δ 7.47 – 7.42 (m, 1H), 6.66 – 6.61 (dd, J = 9.9, 2.4 Hz, 1H), 5.49 – 5.31 (s, 0.5H), 5.21 – 5.06 (m, 0.5H), 5.01 – 4.88 (m, 0.5H), 4.56 – 4.39 (m, 0.5H), 4.22 – 4.15 (m, 2.5H), 3.21 – 2.91 (m, 2.5H), 1.55 – 1.47 (m, 13.5H), 1.18 – 1.13 (d, J = 7.0 Hz, 1.5H). MS (ESI) mass calcd. for $C_{16}H_{24}N_6O_2$ $[M+H]^+$, 332.4; m/z found, 333.1 $[M+H]^+$.

Steps 2-3. The title compound was prepared using the Boc deprotection and General amide coupling conditions as described for **26** (266 mg, 70% over 2 steps). Compound **32** was isolated from the regioisomer by SFC (Stationary phase: CHIRALCEL OJ-H 5µm 250x20mm), Mobile phase: 85% CO_2, 15% iPrOH) (114 mg, 43%). Mp 67.78-71.37 °C. ^{1}H NMR (500 MHz, $CDCl_3$)

δ 7.82 – 7.72 (m, 1H), 7.57 – 7.38 (m, 3H), 6.72 – 6.63 (m, 1H), 5.86 – 5.61 (m, 1H), 4.62 – 4.03 (m, 4H), 3.42 – 2.91 (m, 2H), 1.58 – 1.47 (m, 3H), 1.37 – 1.16 (m, 3H). MS (ESI) mass calcd. for $C_{19}H_{18}ClF_3N_6O$ $[M+H]^+$, 439.1255; m/z found, 439.1258 $[M+H]^+$.

*(S)-(2-Chloro-3-(trifluoromethyl)phenyl)(1-(1-ethyl-1H-pyrazol-5-yl)-6-methyl-1,4,6,7-tetrahydro-5H-[1,2,3]triazolo[4,5-c]pyridin-5-yl)methanone (**33**)*. The compound was prepared in analogy to **32** and the regioisomers were separated by SFC (Stationary phase: CHIRALCEL OJ-H 5µm 250x20mm), Mobile phase: 88% CO_2, 12% iPrOH). ^{1}H NMR (500 MHz, $CDCl_3$) δ 7.83 - 7.76 (m, lH), 7.67 - 7.60 (m, lH), 7.56 - 7.38 (m, 2H), 6.38 - 6.27 (m, lH), 5.89 - 5.61 (m, lH), 4.63 - 4.05 (m, 4H), 3.17 - 2.35 (m, 2H), 1.44 - 1.36 (m, 3H), 1.34 - 1.15 (m, 3H). MS (ESI) mass calcd. $C_{19}H_{18}ClF_3N_6O$, 438.8; m/z found, 439.3 $[M+H]^+$.

*(S)-(2-Chloro-3-(trifluoromethyl)phenyl)(6-methyl-1-(thiophen-3-yl)-6,7-dihydro-1H-[1,2,3]triazolo[4,5-c]pyridin-5(4H)-yl)methanone (**34**)*.

Step 1. General procedure B was conducted using 3-Azidothiophene[30] to give the intermediates tert-butyl (*S*)-6-methyl-1-(thiophen-3-yl)-1,4,6,7-tetrahydro-5*H*-[1,2,3]triazolo[4,5-*c*]pyridine-5-carboxylate and tert-butyl (*S*)-4-methyl-1-(thiophen-3-yl)-1,4,6,7-tetrahydro-5*H*-[1,2,3]triazolo[4,5-*c*]pyridine-5-carboxylate (80 mg crude, ~5%), ratio of products is 2:3, which was carried forward crude.

Steps 2-3. A Boc deprotection and General amide coupling conditions as described for **26** (37 mg, 39% over 2 steps). Compound **34** was isolated from the regioisomer by SFC (Stationary phase: CHIRALCEL OJ-H 5µm 250x20mm), Mobile phase: 80% CO_2, 20% iPrOH) (11 mg, 31%). ^{1}H NMR (500 MHz, $CDCl_3$) δ 7.83 – 7.75 (m, 1H), 7.56 – 7.37 (m, 5H), 5.87 – 5.63 (m, 1H), 4.64 – 4.04 (m, 2H), 3.38 – 2.58 (m, 2H), 1.38 – 1.14 (m, 3H). MS (ESI) mass calcd. for $C_{18}H_{14}ClF_3N_4OS$ $[M+H]^+$, 427.0602; m/z found, 427.0619 $[M+H]^+$.

*(S)-(3-Fluoro-2-(trifluoromethyl)pyridin-4-yl)(1-(5-fluoropyrimidin-2-yl)-6-methyl-6,7-dihydro-1H-[1,2,3]triazolo[4,5-c]pyridin-5(4H)-yl)methanone (**35**)*. To a solution of **41** (8.04 g, 34.3 mmol) and Hunig's base (12 mL, 69 mmol) in CH_2Cl_2 (85 mL) and DMF (40 mL) were added 3-fluoro-2-(trifluoromethyl)isonicotinic acid (7.90 g, 37.8 mmol) and HATU (15.7 g, 41.1 mmol). The reaction was stirred for 30 min then poured into ice water (400 mL). Ethyl acetate was added (400 mL) and the layers were separated. The water layer was extracted with EtOAc (250 mL) 2x. The organic layers were combined and washed with 5% aq LiCl (100 mL) then dried ($MgSO_4$) and purified by flash chromatography (0-85% EtOAc/hexanes gradient) to give the title compound as a white powder (12.7 g, 87%). ^{1}H NMR (500 MHz, $CDCl_3$) δ 8.84 – 8.69 (m, 2H), 8.68 – 8.57 (m, 1H), 7.71 – 7.49 (m, 1H), 5.90 – 5.68 (d, *J* = 16.4 Hz, 0.5H), 5.66 – 5.54 (m, 0.5H), 4.76 – 4.58 (d, *J* = 15.8 Hz, 0.5H), 4.58 – 4.48 (m, 0.5H), 4.45 – 4.33 (m, 0.5H), 4.20 – 4.09 (m, 0.5H), 3.56 – 3.12 (m, 2H), 1.48 – 1.18 (m, 3H). ^{13}C NMR (151 MHz, $CDCl_3$) δ 162.35, 161.96, 157.73, 157.68, 155.96, 155.92, 153.35, 151.59, 151.57, 151.27, 151.25, 139.61, 139.11, 136.90, 136.81, 134.33, 134.23, 133.91, 133.80, 131.29, 129.78, 126.66, 121.30, 119.48, 117.65, 77.28, 49.35, 43.38, 40.13, 40.09, 36.24, 36.12, 30.46, 29.30, 18.64, 17.43. MS (ESI) mass calcd for $C_{17}H_{12}F_5N_7O$ $[M+H]^+$, 426.1096 m/z found, 426.1105 $[M+H]^+$. Specific rotation: $[\alpha]^{20}_D$ +32.1 (c 1.04, CH_3OH).

*(S)-(3-Chloro-2-(trifluoromethyl)pyridin-4-yl)(1-(5-fluoropyrimidin-2-yl)-6-methyl-6,7-dihydro-1H-[1,2,3]triazolo[4,5-c]pyridin-5(4H)-yl)methanone (**36**)*. The title compound was prepared as described for **35** (90 mg, 73%). ^{1}H NMR (500 MHz, $CDCl_3$) δ 8.81 – 8.63 (m, 3H), 7.53 – 7.46 (m, 0.5H), 7.39 (d, *J* = 4.7 Hz, 0.5H), 5.87 – 5.77 (m, 0.5H), 5.68 – 5.58 (m, 0.5H), 4.69 – 4.62 (m, 0.3H), 4.50 – 4.35 (m, 1.2H), 4.08 – 3.96 (m, 0.5H), 3.56 – 3.12 (m, 2H), 1.43 –

1.18 (m, 3H). MS (ESI) mass calcd for $C_{17}H_{12}ClF_4N_7O$ $[M+H]^+$, 442.0801 m/z found, 442.0804 $[M+H]^+$.

*(S)-(1-(5-Fluoropyrimidin-2-yl)-6-methyl-6,7-dihydro-1H-[1,2,3]triazolo[4,5-c]pyridin-5(4H)-yl)(3-methyl-2-(trifluoromethyl)pyridin-4-yl)methanone (**37**)*. The title compound was prepared as described for **35** (32 mg, 27%). ^{1}H NMR (400 MHz, $CDCl_3$) δ 8.81 – 8.71 (m, 2H), 8.68 – 8.55 (m, 1H), 7.40 – 7.19 (m, 1H), 5.91 – 5.77 (m, 0.5H), 5.71 – 5.60 (m, 0.5H), 4.52 – 4.32 (m, 1.5H), 4.11 – 3.99 (m, 0.5H), 3.54 – 3.09 (m, 2H), 2.57 – 2.20 (m, 3H), 1.40 – 1.22 (m, 3H). MS (ESI) mass calcd $C_{18}H_{15}F_4N_7O$, 421.1 m/z found, 422.1 $[M+H]^+$.

*(S)-(1-(5-Fluoropyrimidin-2-yl)-6-methyl-6,7-dihydro-1H-[1,2,3]triazolo[4,5-c]pyridin-5(4H)-yl)(3-methyl-2-(trifluoromethyl)pyridin-4-yl)methanone (**38**)*. The title compound was prepared as described for **35** (16 mg, 21%). ^{1}H NMR (400 MHz, $CDCl_3$) δ 8.80 – 8.70 (m, 2H), 8.68 – 8.55 (m, 1H), 7.40 – 7.20 (m, 1H), 5.92 – 5.81 (m, 0.5H), 5.71 – 5.59 (m, 0.5H), 4.53 – 4.32 (m, 1.5H), 4.12 – 3.97 (m, 0.5H), 3.54 – 3.10 (m, 2H), 2.58 – 2.19 (m, 3H), 1.41 – 1.22 (m, 3H). MS (ESI) mass calcd for $C_{18}H_{15}F_4N_7O$ $[M+H]^+$, 422.1347 m/z found, 422.1359 $[M+H]^+$.

*(S)-(3-Chloro-2-(trifluoromethyl)pyridin-4-yl)(1-(1-ethyl-1H-pyrazol-3-yl)-6-methyl-6,7-dihydro-1H-[1,2,3]triazolo[4,5-c]pyridin-5(4H)-yl)methanone (**39**)*. The Boc deprotection and General amide coupling conditions were conducted as described for **26** from *tert*-butyl (*S*)-1-(1-ethyl-1*H*-pyrazol-3-yl)-6-methyl-1,4,6,7-tetrahydro-5*H*-[1,2,3]triazolo[4,5-*c*]pyridine-5-carboxylate and *tert*-butyl (*S*)-1-(1-ethyl-1*H*-pyrazol-3-yl)-4-methyl-1,4,6,7-tetrahydro-5*H*-[1,2,3]triazolo[4,5-*c*]pyridine-5-carboxylate (108 mg, 16% over 2 steps). Compound **39** was isolated from its regioisomer by SFC (Stationary phase: CHIRALPAK AD-H 5µm 250x20mm), Mobile phase: 85% CO_2, 15% MeOH) (52 mg, 48%). ^{1}H NMR (500 MHz, $CDCl_3$) δ 8.72 – 8.61 (m, 1H), 7.51 – 7.35 (m, 2H), 6.73 – 6.65 (m, 1H), 5.85 – 5.57 (m, 1H), 4.65 – 3.95 (m, 4H),

3.43 – 2.97 (m, 2H), 1.57 – 1.20 (m, 6H). MS (ESI) mass calcd. for $C_{18}H_{17}ClF_3N_7O$ $[M+H]^+$, 440.1208; m/z found, 440.1222 $[M+H]^+$.

*(S)-(3-Fluoro-2-(trifluoromethyl)pyridin-4-yl)(1-(5-hydroxypyrimidin-2-yl)-6-methyl-6,7-dihydro-1H-[1,2,3]triazolo[4,5-c]pyridin-5(4H)-yl)methanone (**40**)*. ^{1}H NMR (500 MHz, $CDCl_3$) δ 8.66 – 8.54 (m, 1H), 8.46 – 8.32 (m, 2H), 7.65 – 7.54 (m, 1H), 6.78 – 5.95 (br m, 1H), 5.75 – 5.49 (m, 1H), 4.70 – 4.04 (m, 2H), 3.44 – 3.09 (m, 2H), 1.39 – 1.14 (m, 3H). MS (ESI) mass calcd. for $C_{17}H_{13}F_4N_7O_2$ $[M+H]^+$, 424.1140; m/z found, 424.1150 $[M+H]^+$.

Primary pharmacological assays. Lipopolysaccharide (LPS)-primed, Bz-ATP induced IL-1β release from human peripheral blood mononuclear cells (PBMC) was used as the primary screen to test for P2X7 antagonism and was conducted as previously described.[28,29] Ca^{2+} flux and radioligand binding assays were conducted with 1321N1 cells expressing the recombinant human P2X7 channel as previously described.[28,29]

DMPK. General Methods. A 10 mM compound stock solution in DMSO further diluted in acetonitrile/water to yield a secondary 1 mM solution was used in all in vitro assays. Pooled human liver microsomes of mixed gender, mouse, rat, beagle dog, and cynomolgus monkey of male gender were purchased from BD Gentest (Woburn, MA). Plasma from various species was purchased from Bioreclamation, Inc. (Westbury, NY). All other commercially available reagents and solvents were either analytical or HPLC grade. In vitro and PK samples were analyzed by LC−MS/MS in the multiple reaction monitoring (MRM) scan mode with electrospray ionization (ESI). The following DMPK assays were conducted as previously reported:[11] Caco-2 Permeability, Solubility in Aqueous Systems, Cocktail CYP Inhibition Assay, CYP3A Time Dependent Inhibition (TDI), plasma protein binding. Microsomal stability studies were conducted on a Biomek® FX Robotic Liquid Handling Workstation (Beckman Coulter, Brea,

CA) as previously described.[11] The extraction ratio (ER) was calculated by dividing the predicted hepatic clearance by species blood flow (Q), where Q is 55, 21, 31 and 44 mL/min/kg for rat, human, dog and monkey respectively.

hERG QPatch™. Experiments were performed using CHO cells stably expressing the hERG potassium channel. Cells were grown at 37°C and 5% CO_2 in culture flasks in Ham's F12 Medium supplemented with 10% heat-inactivated fetal calf serum, hygromycin B (100 µg/ml) and geneticin (100 µg/ml). For use in the automated patch-clamp system QPatch (Sophion) cells were harvested to obtain cell suspension of single cells. Solutions: The bath solution contained (in mM) 145 NaCl, 4 KCl, 10 glucose, 10 HEPES, 2 $CaCl_2$ and 1 $MgCl_2$ (pH 7.4 with NaOH). The pipette solution contained (in mM) 120 KCl, 10 EGTA, 10 HEPES, 5.374 $CaCl_2$ and 1.75 $MgCl_2$ (pH 7.2 with KOH. Patch-clamp experiments were performed in the voltage-clamp mode and whole-cell currents were recorded with an automated patch-clamp assay utilizing the QPatch system (Sophion). Current signals were amplified and digitized, stored and analyzed by using the QPatch assay software. The holding potential was -80 mV. The hERG current (K+-selective outward current) was determined as the maximal tail current at -40 mV after a 2 second depolarization to +60 mV. Pulse cycling rate was 15 s. A short pulse (90 ms) to -40 mV served as a baseline step to calculate the tail current amplitude. After establishing whole-cell configuration and a stability period, the vehicle was applied for 5 minutes followed by the test substance by increasing concentrations of 10^{-7} M, 3 x 10^{-7} M and 3 x 10^{-6} M. Each concentration of the test substance was applied twice. The effect of each concentration was determined after 5 min as an average current of 3 sequential voltage pulses. To determine the extent of block the residual current was compared with vehicle pre-treatment. Data are presented as mean values ± standard error of the mean (SEM).

In vivo pharmacokinetic studies. Single dose PK studies in preclinical species (male Balb/c mice, Sprague Dawley rats, beagle dogs, or cynomolgus monkeys) were conducted following i.v. and p.o. administration as a solution in the vehicles indicated. Blood was sampled at predose and at 0.033 (i.v.), 0.083 (i.v.), 0.25, 0.5, 1, 2, 4, 6, 8, and 24 h postdose. In dogs, instead of 6 and 8 h time points blood was drawn at 7 h. Plasma concentrations were quantitated by LC−MS/MS. PK parameters were derived from noncompartmental analysis of the plasma concentration vs time data using WinNonlin software (Pharsight, Palo Alto, CA).

Ex vivo radioligand binding autoradiography. Animal work was done in accordance with the Guide Care for and Use of Laboratory Animals adopted by the US National Institutes of Health. Animals were allowed to acclimate for 7 days after receipt. They were group housed in accordance with institutional standards, received food and water ad libitum and were maintained on a 12 hour light/dark cycle. Male Sprague Daley Rats approximately 300-400 grams in body weight were used. For time course studies 2 animals per time point over 3 time points were used. For dose response studies, three animals per dose over 7-10 doses were tested. Animals were euthanized with carbon dioxide and plasma and tissue removed. Tissue sections were prepared as previously described.[28,29]

1- and 4-Day repeat dose oral toxicology studies. For the repeat dose toxicology group, animals were administered at oral doses described in the text for 4 days, with necropsy performed on day five. The tissues from control and treated groups were embedded in paraffin, processed into slides by sectioning at 4 μm, stained with hematoxylin and eosin, and examined microscopically.

ASSOCIATED CONTENT:

Supporting Information Available: Molecular formula strings, synthesis of acid chloride, azide intermediates and **30, 31** and **40**, crystallography experiments for **29**, Log D and pK_a measurements for **35**, CYP data for **29** and **35**, experimental protocols and data for HR-XPRD, digital imaging, DSC and TGMS for **29** and **35**, thermal and shock stability screen results for 2-azido-5-fluoropyrimidine. This material is available free of charge via the Internet at http://pubs.acs.org.

AUTHOR INFORMATION:
Corresponding Author
*E-mail: cchrovia@its.jnj.com

Author Contributions

The manuscript was written through contributions of all authors. All authors have given approval to the final version of the manuscript.

ACKNOWLEDGEMENTS:

The authors would like to thank Hong Ao and Xi Wang for in vitro pharmacology assays, Jennifer Ingram-Ross, Judith Herrlich and Stewart Bryant for their work in the preclinical toleration studies, Brigitte Loenders and Vijay Urmaliya for their work in the preclinical cardiovascular safety studies, Heather Mcallister for analytical support, Curtis Moore for x-ray diffraction studies, Crystallics for polymorph screens, David Speybrouck for enabling the separation of regioisomers, Khoa Tran for HRMS data, Pascal Bonaventure for helpful manuscript suggestions and Greg Chen, Jimmy Liang and Dave Kummer for valuable reaction suggestions.

ABBREVIATIONS:

ADME, absorption, distribution, metabolism and excretion, ALT, Alanine Aminotransferase, AUC, area under the curve, BCS, Biopharmaceutical Classification System, Bz-ATP, 2'(3')-O-(4-Benzoylbenzoyl)adenosine-5'-triphosphate, CD, Crohn's disease, CHO, Chinese hampster ovary, CL, clearance, CNS, central nervous system, *m*-CPBA, *meta*-chloroperbenzoic acid, CYP Cytochrome P450, EC, effective concentration, ED, effective dose, EGTA, ethyleneglycol-bis(2-aminoethylether)-*N,N,N′,N′*-tetraacetic acid, ER, extraction ratio, F, bioavailability, FIH, first in human, HATU, [(Dimethylamino)-1*H*-1,2,3-triazolo-[4,5-*b*]pyridin-1-ylmethylene]-*N*-methylmethanaminium hexafluorophosphate *N*-oxide, HEPES, 4-(2-Hydroxyethyl)piperazine-1-ethanesulfonic acid, Het, heterocycle, HP-β-CD, (2-Hydroxypropyl)-β-cyclodextrin, IC, inhibitory concentration, IL-1β, interleukin-1β, i.v., intravenous, NOAEL, no adverse event level, PEG400, Polyethylene Glycol 400, PFTBA, perfluorotributylamine, PK, pharmacokinetics, p.o., per os, PoC, proof of concept, q.d., quaque die (once a day), RA, Rheumatoid Arthritis, SAR, structure-activity relationship, SFC, supercritical fluid chromatography, *p*-TSA, *para*-toluenesulfonic acid, V_{ss}, volume of distribution, VT, variable temperature.

REFERENCES:

(1) Jones, K. A.; Thomsen, C. The role of the innate immune system in psychiatric disorders. *Mol. Cell. Neurosci*. **2013**, *53*, 52–62.

(2) Dinarello, C.A. Immunological and inflammatory functions of the interleukin-1 family. *Annu. Rev. Immunol*. **2009**, *27*, 519–550.

(3) Bhattacharya, A.; Savall, B.; Lord, B.; Bonaventure, P.; Aluisio, L.; Koudriakova, T.; Sepassi, K.; Schoetens, F.; Ceusters, M.; Carruthers, N.; Lovenberg, T.; Letavic, M. JNJ-54175446, A CNS penetrant P2X7 antagonist in clinical development for mood disorders. *Neuropsychopharmacology* **2016**, *41*, S289–S454.

(4) Iwata, M.; Ota, K. T.; Li, X.-Y.; Sakaue, F.; Li, N.; Dutheil, S.; Banasr, M.; Duric, V.; Yamanashi, T.; Kaneko, K.; Rasmussen, K.; Glasebrook, A.; Koester, A.; Song, D.; Jones, K. A.; Zorn, S.; Smagin, G.; Duman, Ronald S. Psychological stress activates the inflammasome via release of ATP and stimulation of the P2X7 receptor. *Biol. Psychiatry* **2016**, *80*, 12-22.

(5) Lovenberg, T.; Aluisio, L.; Ceusters, M.; Letavic, M.; Bhattacharya, A. Characterization of P2X7 antagonists in the rodent brain: Promise for a novel mechanism of action for mood disorder? *Proceedings of the CINP Thematic Meeting on Stress, Inflammation and Depression: Focus on Novel Antidepressant Targets*, Dublin, Ireland, June 4-6, 2015.

(6) Eser, A.; Colombel, J.-F.; Rutgeerts, P.; Vermeire, S.; Vogelsang, H.; Braddock, M.; Persson, T.; Reinisch, W. Safety and efficacy of an oral inhibitor of the purinergic receptor P2X7 in adult patients with moderately to severely active crohn's disease: a randomized placebo-controlled, double-blind, phase IIa study. *Inflamm. Bowel Dis*. **2015**, *21*, 2247-2253.

(7) Keystone, E. C.; Wang, M. M.; Layton, M.; Hollis, S.; McInnes, I. B. Clinical evaluation of the efficacy of the P2X7 purinergic receptor antagonist AZD9056 on the signs and symptoms of rheumatoid arthritis in patients with active disease despite treatment with methotrexate or sulphasalazine. *Ann. Rheum. Dis*. **2012**, *71*, 1630–1635.

(8) Stock, T. C.; Bloom, B. J.; Wei, N.; Ishaq, S.; Park, W.; Wang, X.; Gupta, P.; Mebus, C. A. Efficacy and safety of CE-224,535, an antagonist of P2X7 receptor, in treatment of patients with rheumatoid arthritis inadequately controlled by methotrexate. *J. Rheumatol*. **2012**, *39*, 720−727.

(9) Letavic, M. A; Savall, B. M.; Allison, B. B.; Aluisio, L.; Andres, J. I.; De Angelis, M.; Ao, H.; Beauchamp, D.; Bonaventure, P.; Bryant, S.; Carruthers, N. I., Ceusters M.; Coe, K.; Dvorak, C. A.; Fraser, I.; Gelin, C. F.; Koudriakova, T.; Liang, J.; Lord, B.; Lovenberg, T.; Otieno, M.; Schoetens, F.; Swanson, D.; Wang, X.; Wickenden, A.; Bhattacharya, A. 4-Methyl-6,7-dihydro-4*H*-triazolo[4,5-c]pyridine-based P2X7 receptor antagonists: optimization of pharmacokinetic properties leading to the identification of a clinical candidate. *J. Med. Chem.* **2017**, *60*, 4559-4572.

(10) Rudolph, D. A.; Alcazar, J.; Ameriks, M. K.; Anton, A. B.; Ao, H.; Bonaventure, P.; Carruthers, N. I.; Chrovian, C. C.; De Angelis, M.; Lord, B.; Rech, J. C.; Wang, Q.; Bhattacharya, A.; Andres, J. I.; Letavic, M. A. Novel methyl substituted 1-(5,6-dihydro-[1,2,4]triazolo-[4,3-a]pyrazin-7(8H)-yl)methanones are P2X7 antagonists. *Bioorg. Med. Chem. Lett.* **2015**, *25*, 3157−3163.

(11) Swanson, D. M.; Savall, B. M.; Coe, K. J.; Schoetens, F.; Koudriakova, T.; Skaptason, J.; Wall, J.; Rech, J.; Deng, X.; De Angelis, M.; Everson, A.; Lord, B.;Wang, Q.; Ao, H.; Scott, B.; Sepassi, K.; Lovenberg, T. W.; Carruthers, N. I.; Bhattacharya, A.; Letavic, M. A. Identification of (R)-(2-chloro-3-(trifluoromethyl)phenyl)(1-(5-fluoropyridin-2-yl)-4-methyl-6,7-dihydro-1H-imidazo[4,5-c]pyridin-5(4H)-yl)methanone (JNJ 54166060), a small molecule antagonist of the P2X7 receptor. *J. Med. Chem.* **2016**, *59,* 8535-8548.

(12) Chrovian, C. C.; Soyode-Johnson, A.; Ao, H.; Bacani, G. M.; Carruthers, N. I.; Lord, B.; Nguyen, L.; Rech, J. C.; Wang, Q.; Bhattacharya, A.; Letavic, M. A. Novel phenyl-substituted 5,6-dihydro-[1,2,4]triazolo[4,3-a]pyrazine P2X7 antagonists with robust target engagement in rat brain. *ACS Chem. Neurosci*. **2016**, *7*, 490−497.

(13) Savall, B. M.; Wu, D.; De Angelis, M.; Carruthers, N. I.; Ao, H.; Wang, Q.; Lord, B.; Bhattacharya, A.; Letavic, M. A. Synthesis, SAR, and pharmacological characterization of brain penetrant P2X7 receptor antagonists. *ACS Med. Chem. Lett*. **2015**, *6*, 671−676.

(14) Ameriks, M. K.; Ao, H.; Carruthers, N. I.; Lord, B.; Ravula, S.; Rech, J. C.; Savall, B. M.; Wall, J. L.; Wang, Q.; Bhattacharya, A.; Letavic, M. A. Preclinical characterization of substituted 6,7-dihydro-[1,2,4]triazolo[4,3-a]pyrazin-8(5H)-one P2X7 receptor antagonists. *Bioorg. Med. Chem. Lett*. **2016**, *26*, 257−261.

(15) Ziff, J.; Rudolph, D. A.; Stenne, B.; Koudriakova, T.; Lord, B.; Bonaventure, P.; Lovenberg, T. W.; Carruthers, N. I.; Bhattacharya, A.; Letavic, M. A.; Shireman, B. T. Substituted 5,6-(dihydropyrido[3,4-d]pyrimidin-7(8H)-yl)-methanones as P2X7 antagonists. *ACS Chem. Neurosci*. **2016**, *7*, 498−504.

(16) Kolb, H. C.; Finn, M. G.; Sharpless, K. B. Click chemistry: diverse chemical function from a few good reactions. *Angew. Chem., Int. Ed*. **2001**, *40*, 2004-2021.

(17) Deng, X.; Liang, J.; Allison, B. B.; Dvorak, C.; McAllister, H.; Savall, B. M.; Mani, N. S. Allyl-assisted, Cu(I)-catalyzed azide-alkyne cycloaddition/allylation reaction: assembly of the [1, 2,3]triazolo-4,5,6,7-tetrahydropyridine core structure. *J. Org. Chem.* **2015**, *80*, 11003-11012.

(18) Lin, Yibei; Chen, Yali; Ma, Xuyan; Xu, Di; Cao, Weiguo; Chen, J. Aryne click chemistry: synthesis of oxadisilole fused benzotriazoles or naphthotriazoles from arynes and azides. *Tetrahedron* **2011**, *67*, 856-859.

(19) Zhang, F.; Moses, J. E. Benzyne click chemistry with in situ generated aromatic azides. *Org Lett.* **2009,**1587-1590.

(20) Chen, M.; Buchwald, S. L. Continuous-flow synthesis of 1-substituted benzotriazoles from chloronitrobenzenes and amines in a C-N bond formation /hydrogenation/diazotization /cyclization sequence. *Angew Chem. Int. Ed*. **2013**, *52*, 4247-4250.

(21) Huisgen, R.; Szeimies, G.; Mobius, L. K1.3-Dipolare cycloadditionen, XXXII. Kinetik der additionen organischer azide an CC-mehrfachbindungen. *Chem. Ber*. **1967**, *100*, 2494–2507.

(22) Ramachary, D. B.; Ramakumar, K.; Narayana, V. V. Amino acid-catalyzed cascade [3+2]-cycloaddition/hydrolysis reactions based on the push-pull dienamine platform: synthesis of highly functionalized NH-1,2,3-triazoles. *Chem Eur J.* **2008**, *7*, 9143-9147.

(23) Belkheira, M.; El Abed, D.; Pons, J.-M.; Bressy, C. Organocatalytic synthesis of 1,2,3-triazoles from unactivated ketones and arylazides. *Chem. Eur. J.* **2011**, *17*, 12917-12921.

(24) Dean, D. K.; Munoz-Muriedas, J.; Sime, M.; Steadman, J. G. A.; Thewlis, R. E. A.; Trani, G.; Walter, D. S. 5,6,7,8-tetrahydro[1,2,4]triazolo[4,3-a]pyrazine derivatives as P2X7 modulators. WO 2010125102 A1 20101104, November 4, 2010.

(25) Parsons, S.; Flack, H. D. Precise absolute-structure determination in light-atom crystals. *Acta Crystallogr., Sect. A: Found. Crystallogr.* **2004**, *60*, s61.

(26) Discovery-stage recrystallization techniques employed: cooling-evaporation crystallization (25 solvent pairs), cooling crystallization with hot filtration (14 solvent pairs), crash-crystallization by anti-solvent addition (15 solvent pairs), evaporative crystallization (15 solvent pairs), long term slurry conversion (10 solvents) and thermocycling (15 solvents). Vapor diffusion techniques and thermocycling and polymer assisted crystallization were also attempted.

(27) Mahmood, I.; Balian, J. D. Interspecies scaling: predicting clearance of drugs in humans: three different approaches. *Xenobiotica* **1996**, *26,* 887-895.

(28) Bhattacharya, A.; Wang, Q.; Ao, H.; Shoblock, J. R.; Lord, B.; Aluisio, L.; Fraser, I.; Nepomuceno, D.; Neff, R. A.; Welty, N.; Lovenberg, T. W.; Bonaventure, P.; Wickenden, A. D.; Letavic, M. A. Pharmacological characterization of a novel centrally permeable P2X7 receptor antagonist: JNJ-47965567. *Br. J. Pharmacol*. **2013**, *170*, 624-640.

(29) Lord, B.; Ameriks, M. K.; Wang, Q.; Fourgeaud, L.; Vliegen, M.; Verluyten, W.; Haspeslagh, P.; Carruthers, N. I.; Lovenberg, T. W.; Bonaventure, P.; Letavic, M. A.; Bhattacharya, A. A novel radioligand for the ATP-gated ionchannel P2X7:[^{3}H] JNJ-54232334. *Eur. J. Pharmacol.* **2015**, *765*, 551−559.

(30) Potratz, S.; Mishra, A.; Bäuerle, P. Thiophene-based donor–acceptor co-oligomers by copper-catalyzed 1,3-dipolar cycloaddition. *Beilstein J. Org. Chem*. **2012**, *8*, 683–692.

TABLE OF CONTENTS GRAPHIC:

30 mg QD predicted clinical dose for robust P2X7 occupancy

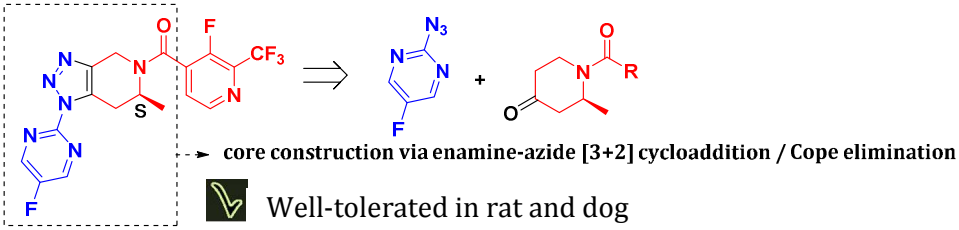

Well-tolerated in rat and dog

Suppresses IL-1β release in freely moving conscious rats